PBL Netherlands Environmental Assessment Agency

PBL Note

The IMAGE model suite used for the OECD Environmental Outlook to 2050

Compiled by:
T. Kram and E. Stehfest

Contributions from:
Rob Alkemade, Lex Bouwman, Hester Biemans, Michel de Elzen, Henk Hilderink, Kees Klein Goldewijk, Tom Kram, Paul Lucas, Jos Olivier, Elke Stehfest, Detlef van Vuuren

PBL publication number 500113002

Introduction

1. This document contains the technical background for the IMAGE model suite to be used for the next OECD Environmental Outlook. It describes the models and modules used and their interconnections. The scenarios and projections for the OECD Environmental Outlook are the result of an integrated analysis of the economy-environment interface, in which, apart from economic factors influencing the environment, ample attention is given to physical factors related with the energy and agriculture sectors (Figure 1).

Figure 1
The modelling scheme applied in the *OECD Environmental Outlook*

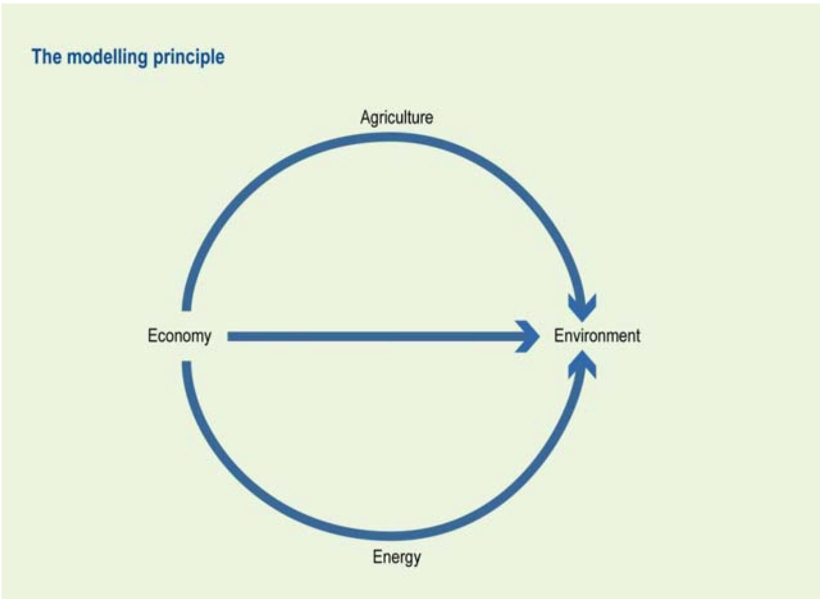

For the analysis a combination of models are being used, connected through harmonized data flows (see Figure 2). Data on economic activities, described by ENV-Linkages, steer the IMAGE and related models. In addition to the simple one-dimensional relation between economic driving forces and changes in the environment, the physical flows of energy and the availability of land are important drivers and sometimes limiting factors to developments in the environment. In this modelling exercise the last have been taken explicitly into account and these two groups of variables have a central position in the modelling framework: next to the link from the economic modelling in ENV-Linkages to IMAGE, energy use is modelled in detail in TIMER, while land use factors are processed through LEITAP. This document provides a summary of the model descriptions to enhance the understanding of the scope and limitations of the modelling exercise. Detailed model descriptions can be found in the referred literature, and in the Background Report for the previous OECD Environmental Outlook to 2030 (MNP and OECD, 2008).

Figure 2
Overview of the IMAGE model suite

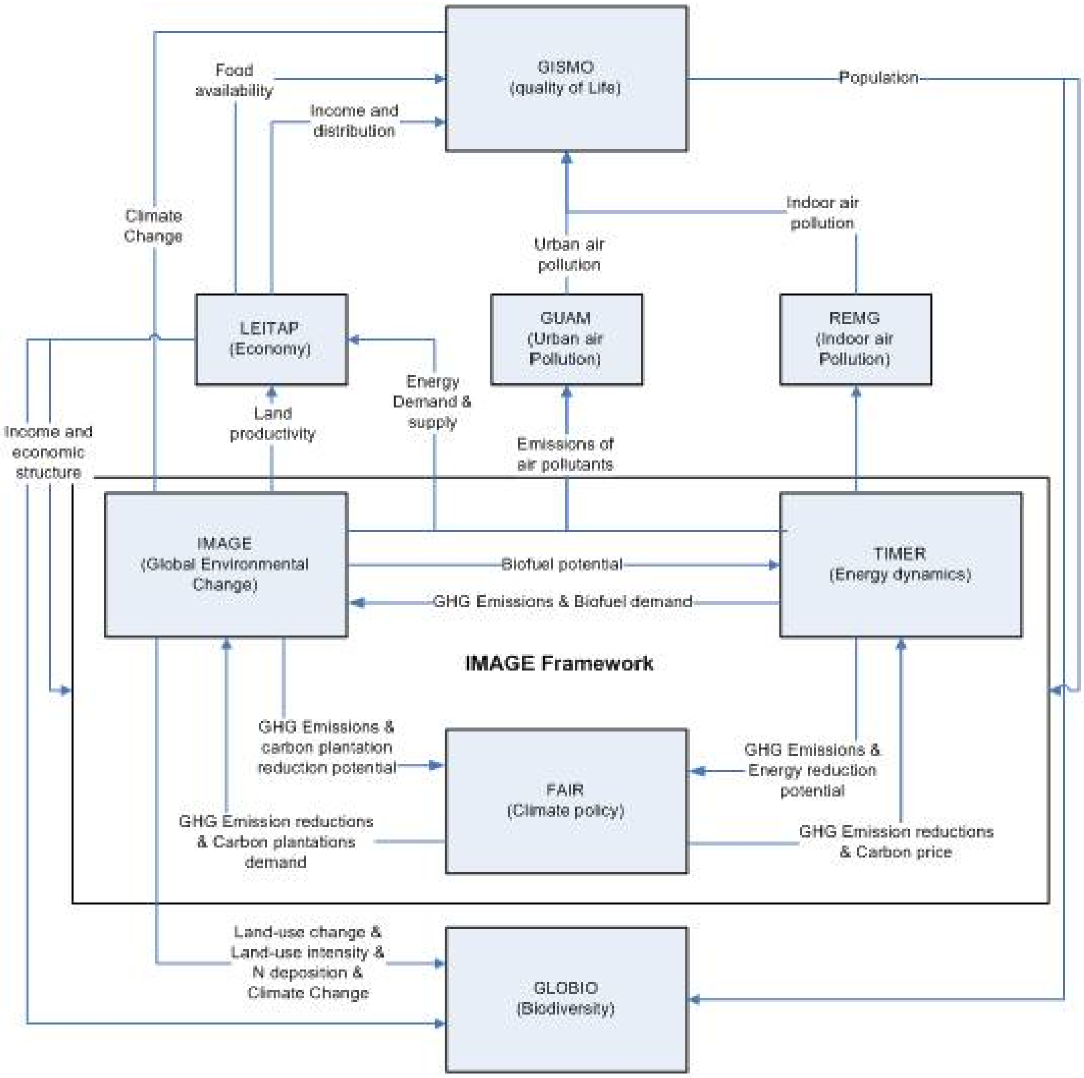

II IMAGE – FRAMEWORK

2. The Integrated Model to Assess the Global Environment (IMAGE) has initially been developed as an integrated assessment model to study anthropocentric climate change (Rotmans, 1990). Later it was extended to include a more comprehensive coverage of global change issues in an environmental perspective (Alcamo *et al.* 1994, IMAGE team, 2001). The current main objectives of IMAGE are to contribute to scientific understanding and support decision-making by quantifying the relative importance of major processes and interactions in the society-biosphere-climate system (see further: http://www.pbl.nl/image).

3. IMAGE provides a dynamic and long-term assessment of the systemic consequences of global change up to 2100. The model was set up to give insight into causes and consequences of global change up to 2100 as a quantitative basis for analysing the relative effectiveness of various policy options for addressing global change. Figure 3 provides an overview of the IMAGE modelling framework used in this analysis.

4. In earlier studies two models associated with, but not integrated in IMAGE, were used to provide basic drivers for the IMAGE model. These are the general equilibrium economy model, WorldScan (CPB, 1999), and the population model, PHOENIX (Hilderink, 2000). The WorldScan model provides input for IMAGE on economic developments, and PHOENIX provides input on demographic developments for both IMAGE and WorldScan.

5. For the OECD Environment Outlook, the population projection is taken from the UN directly and is one of the inputs for the OECD ENV-Linkages model. The economic results from the ENV-linkages model are used as drivers to produce the detailed, physically oriented projections for the energy and land-use sectors by various models in the IMAGE framework. IMAGE uses agricultural demand, production and trade as calculated by the LEITAP model. More aspects of the linkage between the two models are described in Chapter 5.

6. The TIMER model (see Chapter 6) provides regional energy consumption, energy efficiency improvements, fuel substitution, supply and trade of fossil fuels and renewable energy technologies. On the basis of energy use and industrial production TIMER computes emissions of greenhouse gases (GHG), ozone precursors and acidifying compounds.

7. The land and climate module of IMAGE (see Chapter 3) computes land-use changes based on regional production of food, animal feed, fodder, grass and timber, and changes in natural vegetation due to climate change. Consequently, emissions and carbon exchange from land use changes, natural ecosystems and agricultural production systems are calculated. The Atmospheric Ocean System then computes changes in atmospheric composition and climate using these emissions, and the emissions from the TIMER model.

More IMAGE information on: http://www.pbl.nl/en/themasites/image/index.html

Figure 3
Flow diagram of the IMAGE framework

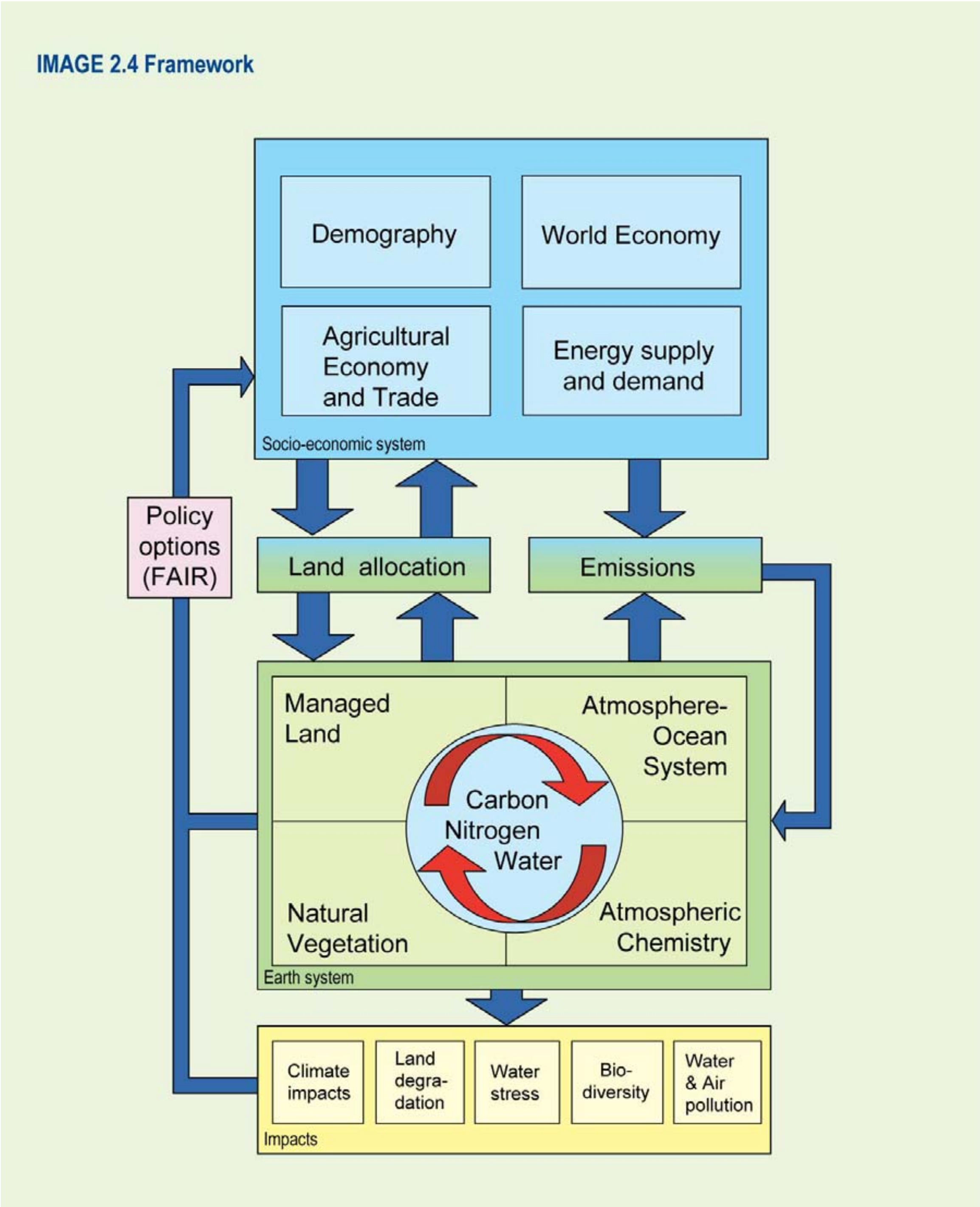

III IMAGE – LAND AND CLIMATE

8. This chapter zooms in on the land and climate module of IMAGE and its sub-systems, as the geographically explicit modelling of land-use is one of the outstanding characteristics of IMAGE. The Terrestrial Vegetation Model (TVM) simulates the potential distribution of natural vegetation and crops on the basis of climate conditions and soil characteristics on a spatial resolution of 0.5 degree latitude by 0.5 degree longitude. It also estimates potential crop productivity, which is used by Land Cover Model (LCM), to determine the allocation of the cropland to different crops. First, TVM calculates 'constraint-free rain fed crop yields' accounting for local climate and light attenuation by the canopy of the crop considered (FAO, 1981). The climate-related crop yields are adjusted for grid-specific conditions by a soil factor with values ranging from 0.1 to 1.0. This soil factor takes into account three soil quality indicators: *(1)* nutrient retention and availability; *(2)* level of salinity, alkalinity and toxicity; and, *(3)* rooting conditions for plants. The adjustment factor is calibrated using historical productivity figures and also includes the fertilization effect of changes in the atmospheric concentration of carbon dioxide. The carbon dioxide fertilization is determined by the Terrestrial Carbon Model (TCM) that distinguishes different parameter settings per land cover type (Leemans *et al.*, 2002). The resulting crop productivity, called 'reduced potential productivity of crops', is used in the land cover model.

9. The objective of the Land Cover Model (LCM) is to simulate global land use and land cover changes by reconciling the land use demand with the land potential. The basic idea of LCM is to allocate crop and livestock production as provided by an agro-economic model like LEITAP (see chapter 4) on grid cells within a world regions until the total demand for this region is satisfied. The allocation of land use types is done at grid cell level on the basis of specific land allocation rules like crop productivity, distance to existing agricultural land, distance to water bodies and a random factor (Alcamo et al., 1998).

10. IMAGE uses the historical data for the 1765-1970 period to initialize the carbon cycle and climate system. Actual simulations cover the period 1970-2050. Data for 1970-2000 are used to calibrate the IMAGE model against FAO data. For the period 2001-2050 the simulations are driven by the input from the TIMER model and LEITAP, and by additional scenario assumptions on *e.g.* technology development, yield improvements and efficiencies of animal production systems.

11. Food security may be threatened by loss of soil productivity as a result of human-induced land degradation. Water erosion is the most important cause of land degradation, and its effects are irreversible. IMAGE includes a qualitative approach to assess the land's sensitivity to water erosion. A qualitative approach is most appropriate, because it is impossible to estimate soil loss rates and effects on plant productivity for different water erosion processes at the scale of the IMAGE model (0.5 by 0.5 degree). A modified version of the Universal Soil Loss Equation (USLE) (Wischmeier, 1978) was used to computed erosion hazard on the basis of the terrain erodibility index (considering slope and soil type), rainfall erosivity and land use/cover. The terrain erodibility index is composed of the soil erodibility index and relief index. The rating of soil characteristics is referred to as soil erodibility, based on soil texture and soil depth. The relief index is a landform characterization derived from a digital elevation model (based on differences in elevation within grid cells). The calculation of the rainfall erosivity is based on the maximum mean monthly rainfall intensity calculated from monthly precipitation and the number of wet days. The land use pressure is based on the land cover simulations of the IMAGE model using index values specific for each crop or land cover type.

12. The actual land degradation strongly depends on the conservation measures taken to prevent soil erosion. The results of the land-degradation model of IMAGE can therefore only be used to identify regions where problems of water erosion may present and where they may be most severe, and how the land's sensitivity to water erosion may change in the future under scenarios of population growth, economic growth, technological development and climate change.

Hydrological modeling

13. Currently, the IMAGE model is extended to better simulate the global terrestrial carbon cycle and natural vegetation distribution, to include a global hydrological model, and to improve the crop modelling (MNP, 2006). This is done by coupling the LPJ model to the IMAGE land module (making it an integral part of IMAGEs "Earth System" as depicted in Figure 4). The LPJmL model, having started as a pure dynamic global vegetation model (Sitch *et al*., 2003), as since then been extended to include managed land (LPJmL, Bondeau *et al.*, 2007), and the hydrological cycle (Gerten *et al.*, 2004). For the hydrological modelling, a routing and irrigation module has been implemented (Rost, *et al*., 2008), and computing efficiency was further improved by parallel clustering (von Bloh, *et al*., 2010). The hydrological model of LPJmL has been systematically validated against discharge observations for 300 globally distributed river basins (Biemans, *et al.*, 2009) and against irrigation water use and consumption (Rost, *et al.*, 2008). By coupling LPJ with its hydrological model, the IMAGE scenarios now can also cover future changes in water availability, agricultural water use and its implications for yields, and an indicator for water stress (typically expressed as demand/availability).

Figure 4
Vertical (top) and horizontal (bottom) water flow in the LPJ model

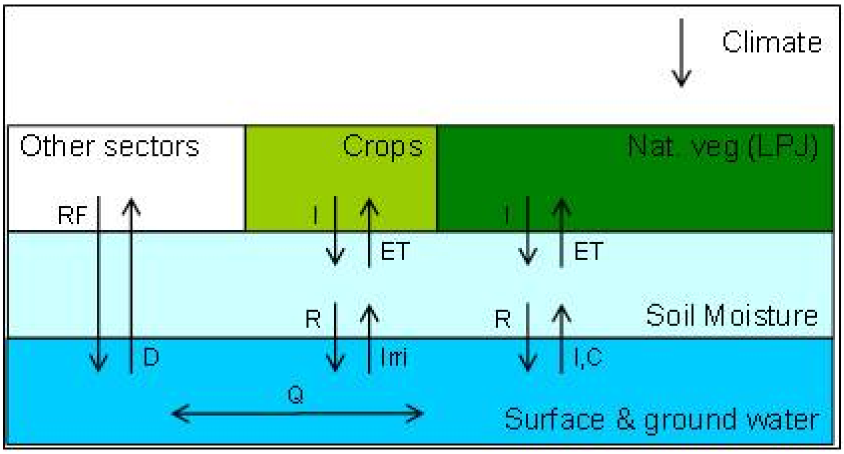

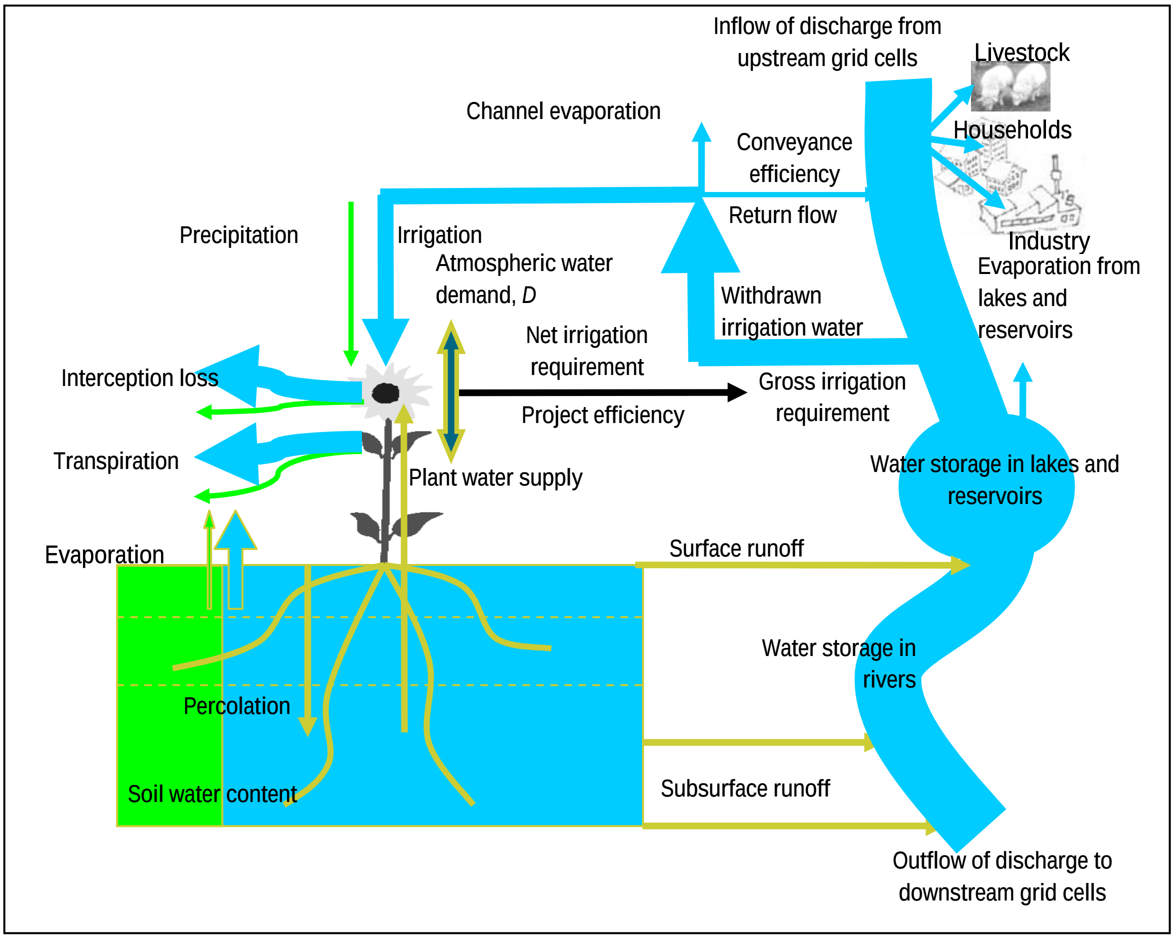

More IMAGE land and climate information on:

http://www.pbl.nl/en/themasites/image/model_details/index.html

IV LEITAP

14. The LEITAP model is a multi-regional, multi-sectoral, static, applied general equilibrium model based on neo-classical microeconomic theory (Nowicki *et al*., 2007 and van Meijl *et al.*, 2006). It is an extended version of the standard GTAP model (Hertel, 1997). The production technology in LEITAP is modeled using a multilevel nested CES production function. In the primary value added nest, the multilevel constant-elasticity-of-substitution (CES) production function describes the substitution of different primary production factors (land, labor, capital and natural resources) and intermediate production factors (*e.g.* energy and animal feed components). The CES nest is also introduced to allow for substitution between different energy sources including biofuels (Banse *et al*., 2008). The model uses fixed input-output coefficients for the remaining intermediate inputs.

15. On the consumption side, the regional household is assumed to distribute income across savings and (government and private) consumption expenditures according to fixed budget shares. Consumption expenditures are allocated across commodities according to a non-homothetic dynamic CDE expenditure function which allows for changes in income elasticities when purchasing power parity (PPP)-corrected real GDP per capita changes. Government expenditures are allocated across commodities according to fixed shares. The commodities consumed by firms, government and households are CES composites of domestic and imported commodities. In addition, imported commodities are differentiated by region of origin using Armington elasticities. Recently, the model has been updated to include biofuels (Banse *et al.*, 2008), and their by-products, and the feed sector for livestock has been improved (Hermosilla *et al*, 2010). To model biofuels use in the fuel production, the nested CES function of the GTAP-E model (Burniaux and Truong, 2002) was adopted and applied for the petrol sector, whereby substitution between crude oil, ethanol and biodiesel is possible via a new intermediate input commodity in petrol sector (called "fuel", being CES aggregate of these liquid fuels). The nested CES structure implies that biofuel demand is determined by the relative prices of crude oil versus ethanol and biodiesel including taxes and subsidies.

16. Regional endowments of labour, capital and natural resources are fixed and fully employed and land supply is modeled by land supply curves (Eickhout *et al.*, 2008), which specify the relationship between land supply and a land rental rate. Labour is divided into two categories: skilled and unskilled. These categories are considered imperfect substitutes in the production process. Land and natural resources are heterogeneous production factors, and this heterogeneity is introduced by using a constant elasticity of transformation (CET) function which allocates these factors among the agricultural sectors. Capital and labour markets are segmented between agriculture and non-agriculture. Labour and capital are assumed to be fully mobile within each of these two groups of sectors, but imperfectly mobile across them. We assume almost perfect substitution between different types of fuels.

Figure 5
Land allocation tree within LEITAP

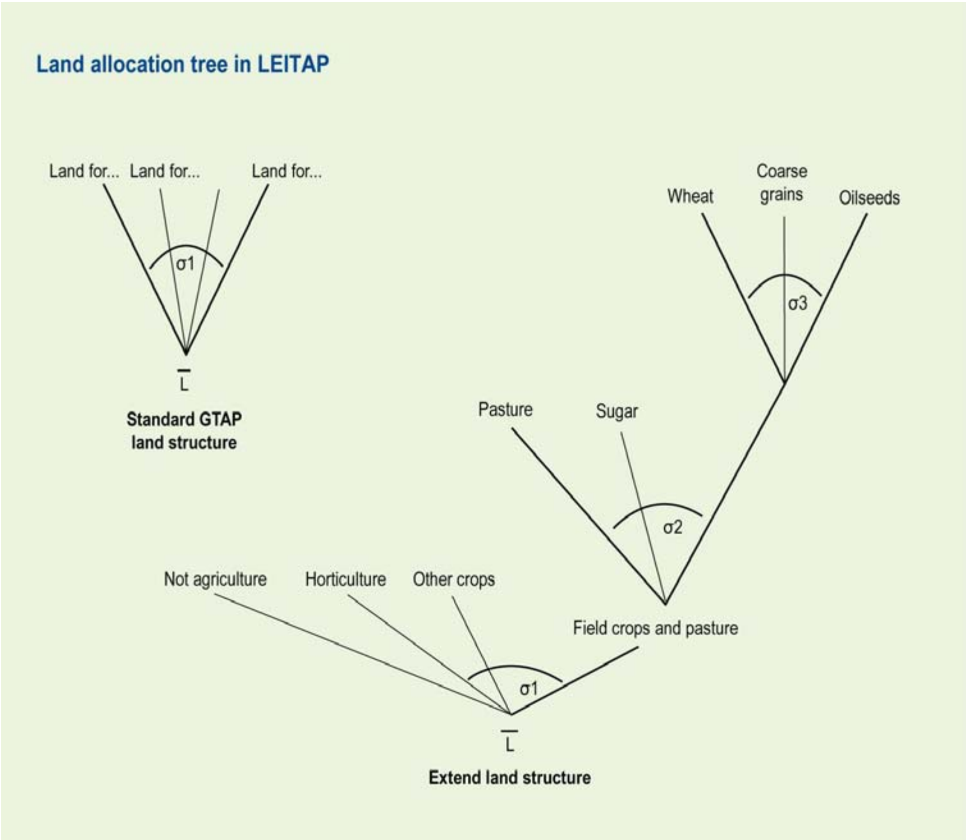

V COUPLING OF LEITAP AND IMAGE

17. The land market in each region is represented in LEITAP by a land supply curve (Figure 6), which specifies the relation between land supply and a rental rate in each region (Eickhout *et al*, 2008). Land that is barely suitable for agriculture in terms of production has been left out of the land supply curve. In regions with ample of idle land (*e.g.* Brazil) suitable for agriculture, marginal costs of taking extra land into production are low, and thus expansion of agricultural area hardly increases the land price. In contrast, regions where almost all available land has been taken into production already (*e.g.* Northern Africa), already have rather high land prices, and would see a strong increase in prices if agricultural land is expanding. A curve depicting the ratio between marginal and average productivity describes the heterogeneity of land. The land supply curve and the productivity curve in LEITAP are consistent with the allocation procedure within IMAGE.

Figure 6
Land supply curve, showing different situation and changes of demand (D), land area in use (l), and rental rate of land (r). L represents the total area suitable for agriculture.

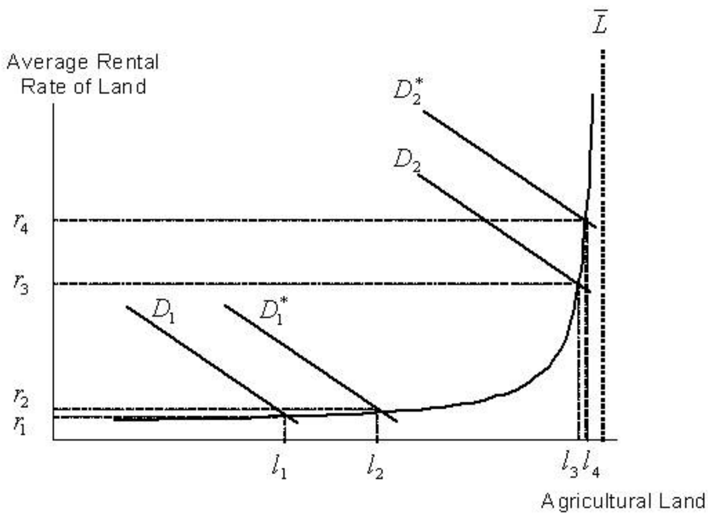

18. Figure 7 shows the methodology of iterating the extended version of LEITAP with IMAGE. The output of LEITAP is, among others, sectoral production growth rates, land use, and a yield factor describing the change in land productivity because of technology improvements and the degree of land intensification. The degree of intensification is modelled endogenously by LEITAP, while the autonomous technological improvement is assumed exogenously using information from FAO's study 'World Agriculture towards 2015/2030' (Bruinsma, 2003).

19. The output from LEITAP is used by the IMAGE model to calculate change in crop productivity, the demand for land, feed efficiency rates and environmental indicators. This procedure delivers adjustments to the achieved changes in yields and changes in feed conversion, which are given back to LEITAP, if necessary. Through this procedure comparable land foresights are simulated in both models.

Figure 7
The modelling framework of LEITAP and IMAGE coupling

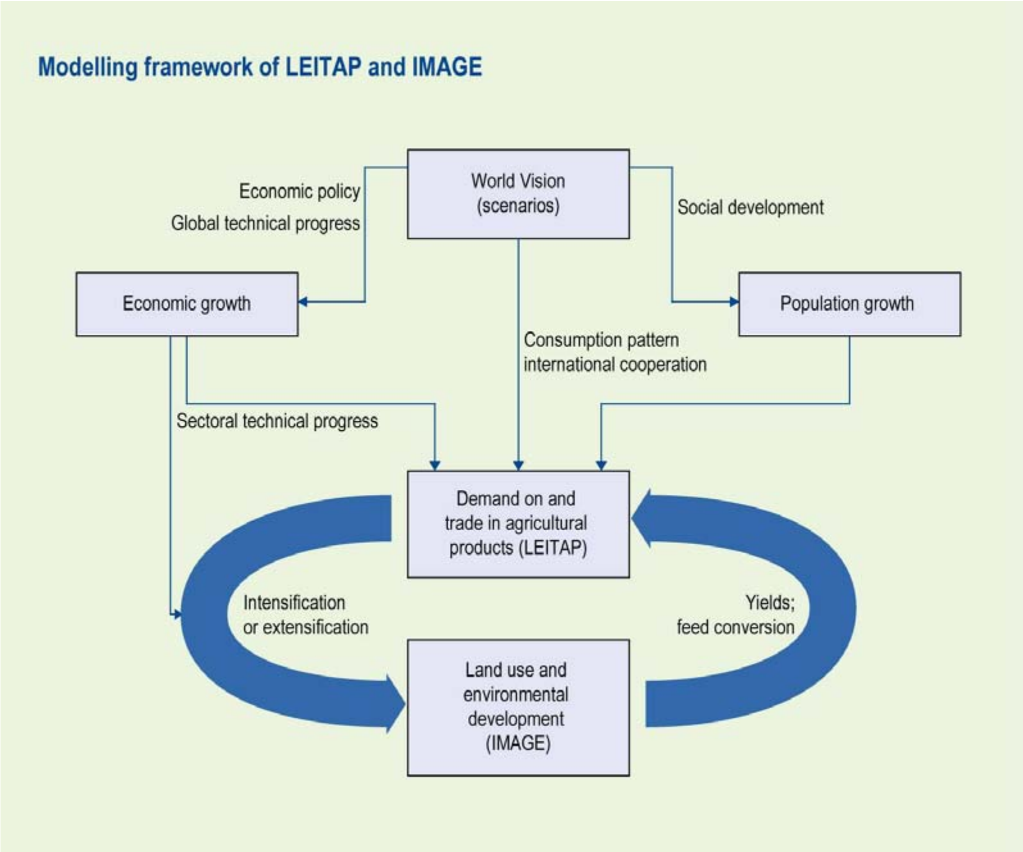

VI TIMER – THE IMAGE ENERGY REGIONAL MODEL

20. The global energy system model TIMER (Targets IMage Energy Regional Model) has been developed to simulate (long-term) energy baseline and mitigation scenarios. The model describes the investments in, and the use of, different types of energy options influenced by technology development (learning-by-doing) and resource depletion. Inputs to the model are macro-economic scenarios and assumptions on technology development, preference levels and restrictions to fuel trade, in this study from ENV-Linkages. The output of the model demonstrates how energy intensity, fuel costs and competing non-fossil supply technologies develop over time. It generates primary and final energy consumption by energy type, sector and region; capacity build-up and utilization, cost indicators and greenhouse gas and other emissions. In TIMER, implementation of mitigation is generally modelled on the basis of price signals (a tax on carbon dioxide). A carbon tax (used as a generic measure of climate policy) induces additional investments in energy efficiency, fossil fuel substitution, and investments in bio-energy, nuclear power, solar power, wind power and carbon capture and storage. Selection of options throughout the model is based on a multinomial logit model that assigns market shares on the basis of production costs and preferences (cheaper, more attractive options get a larger market share; but there is no full optimization) (de Vries *et al.*, 2001).

21. The TIMER model describes the chain from demand for energy services (useful energy) to the supply of energy by different primary energy sources and related emissions (Figure 8). The steps are connected by demand for energy (from left to right) and by feedbacks, mainly in the form of energy prices (from right to left). The TIMER model has three types of submodels: *(i)* the energy demand model; *(ii)* models for energy conversion (electricity and hydrogen production), and *(iii)* models for primary energy supply. Some of the main assumptions for the different sources and technologies are listed in Table 1.

Figure 8
The chain from demand for energy services to related emissions in TIMER

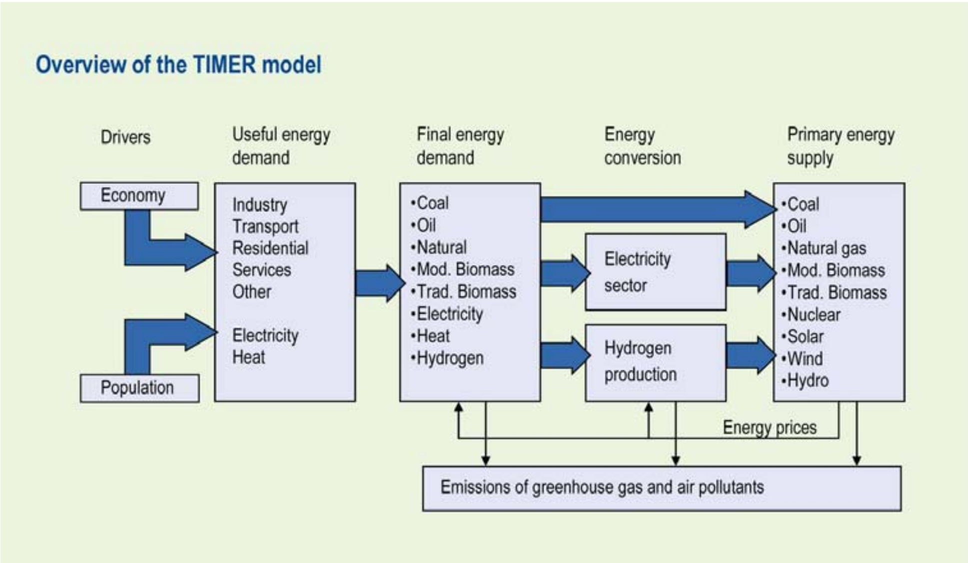

Table 1
Main assumptions in the TIMER model

Option	Assumptions	References
Fossil fuels	Regional resources and production costs for various qualities; the ultimate coal, oil and natural gas resources equal 300, 45, and 117 ZJ, respectively. In time, depletion leads to price increases, while technology change reduces prices. Historical and baseline projections of fossil fuel prices are calibrated against the latest IEA World Energy Outlook.	Rogner (1997), Mulders *et al* (2006)
Carbon capture and storage (CCS)	Regional reservoir availability and storage costs for various options (different categories of empty oil and natural gas reservoirs, coal reservoirs, coal-bed methane recovery, aquifers). Total capacity equals 1500 GtC. Transport and storage costs range, depending on category and region, from 10 to 150 US $/tC.	Hendriks *et al.* (2002)
Power plant efficiency and investment costs	Power plant efficiency and investment costs for 20 types of thermal power plants (coal, oil, natural gas, biomass) including carbon capture and storage defined over time.	Hendriks *et al.* (2004)
Energy crops	Potential and costs for energy crops defined by region on the basis of IMAGE 2 maps (including abandoned agricultural land, natural grasslands and savannah). Primary biomass can be converted into liquid biofuels (for transport) and solid bio-energy (for electricity). Technology development is based on learning-by-doing. Potential depends on future availability of suitable land, and policy assumptions governing their use in light of concerns over biodiversity, deforestation and food prices/food security.	Hoogwijk (2004a)
Solar / wind power	Solar and wind power based on studies that assess global potential on the basis of 0.5 x 0.5 degree maps. Costs change over time as a result of depletion, learning-by-doing and grid penetration (declining capacity credit and excess electricity production).	Hoogwijk (2004b)
Nuclear power	Investment costs of nuclear power based on available information in the literature (most important references indicated). Investment costs are assumed to decrease over time. Fuel costs increase over time as a result of depletion.	MIT (2003); Sims *et al.* (2003)
Hydrogen	Hydrogen modelled on the basis of production from fossil fuels, bio-energy, electricity and solar power (including carbon capture and storage).	Van Ruijven *et al*. (in press)
Energy demand	Parameters for autonomous and price-induced efficiency improvement, and structural change, are mostly based on model calibration.	De Vries *et al.* (2001)

More TIMER information on:

http://www.pbl.nl/en/themasites/image/model_details/energy_supply_demand/Introduction.html

VII FAIR – FRAMEWORK TO ASSESS INTERNATIONAL REGIMES

22. The policy decision-support tool 'Framework to Assess International Regimes for the differentiation of commitments' (FAIR) has been developed to explore and evaluate the environmental and abatement cost implications of various international regimes for differentiation of future commitments for meeting long-term climate targets, such as stabilization of the atmospheric greenhouse gas concentrations (den Elzen, 2005). The model aims to support policy makers by quantitatively evaluating the environmental and costs implications of a range of approaches and linking these to targets for global climate protection. The model was also used to support dialogues between scientists, NGOs and policy makers. To this end the model is set up as an interactive tool with a graphical user interface, allowing for interactive changing and viewing model input and output.

A demonstration version of the model can be downloaded at:

http://www.pbl.nl/en/themasites/fair/download/index.html.

23. The FAIR model consists of three linked models, including a climate model, an emission allocation model and an abatement costs model. The climate model calculates the climate impacts of global emission profiles and emission scenarios, and determines the global emission reduction objective based on the difference between the global emissions scenario (without climate policy) and a global emission profile (including climate policy). The emission allocation model calculates the regional greenhouse gas (GHG) emission allowances for different regimes for the differentiation of future commitments within the context of the global reduction objective from the climate model. The abatement costs model calculates the regional abatement costs and emission levels after trading on the basis of the emission allowances coming from the emission allocation model following a least-cost approach. The model makes full use of the flexible Kyoto mechanisms as emissions trading and substitution of reductions between the different gases and sources.

24. The model calculations are done at the level of 24 IMAGE world regions. The GHG emissions are converted to carbon dioxide equivalent, similar to those in the Kyoto Protocol, *i.e.* the sum of the Global Warming Potential weighted emissions of the six GHGs or groups of GHGs specified in the Kyoto Protocol. Various data sets of historical emissions, baseline scenarios, emission profiles and marginal abatement cost (MAC) curves are included in the model framework to assess the sensitivity of the outcomes to variation in these key inputs.

25. There have been five main developments since the FAIR 2.0 model, which is extensively described in den Elzen and Lucas (2005), *i.e. (i)* the development of multi-gas emission pathways (and envelopes) corresponding to a stabilization of GHG concentration at levels of about 450, 550 and 650 ppm carbon dioxide equivalent (den Elzen *et al.*, 2007; den Elzen & van Vuuren, 2007); *(ii)* abatement cost calculation for mitigation scenarios based on updated MAC curves for all GHG emissions from the TIMER 2.0 model and IMAGE 2.3 model (den Elzen et al., 2008; van Vliet et al., 2009; den Elzen et al., 2011); *(iii)* updated climate attribution calculations (den Elzen *et al.* 2005); *(iv)* an updated Triptych approach at the level of countries (den Elzen *et al.*, 2007), and two additional post-2012 regimes for post-2012 commitments (*i.e.* Common-but-differentiated convergence (Höhne *et al.*, 2006) and the South–North Dialogue Proposal (den Elzen et al., 2007a)); and *(v)* country-scale calculation of emission allowances and abatement costs, referred to as the FAIR-world model (den Elzen, 2005).

26. In recent years a range of extensions and enhancements have been implemented in FAIR in accord with new proposals for global architectures for post-Kyoto agreements. In particular the so-called Copenhagen Pledges are implemented and analyzed for their expected outcome, recognizing the uncertainties contained within the commitments made by parties in their Pledges (den Elzen, 2010).

More information on: http://www.pbl.nl/en/themasites/fair/index.html

VIII GISMO – GLOBAL INTEGRATED SUSTAINABILITY MODEL

27. The Global Integrated Sustainability MOdel (GISMO) is a modelling framework to analyse long-term developments in Quality of Life in relation to social, economic and environmental changes (Hilderink and Lucas, 2008). Quality of Life (its distribution, continuation and improvement) is taken as the main outcome of sustainable development, with health, poverty and education as its main pillars. Indicators being covered by GISMO are for example population health indicators, varying from simple mortality rates to more advanced measures as Disability-Adjusted Life Years (DALY), development indicators, such as the human development index (HDI) and the Millennium Development Goals (MDG).

Modules of GISMO

28. The indicator values are derived from various model components included in GISMO. The main modules of GISMO are:

- a demographic model (PHOENIX) which is a cohort-component population model, including fertility, mortality, migration and urbanization;
- a health model that links mortality and morbidity to socio-economic and environmental risk factors;
- an education model that addresses primary, secondary and tertiary school enrolment and attainment; and
- a poverty model that determines poverty as a result of economic growth and changes in distribution.

29. The GISMO modeling framework links closely to other models, including IMAGE, TIMER and economic models. Inputs from these models are economic impacts, including GDP, consumption and price changes, and environmental health risks, including food availability (undernourishment), climate change (malaria) and indoor and urban air pollution (lung cancer, cardiopulmonary diseases and acute respiratory infections). An overview of interlinkages of GISMO models with the others are presented in Figure 9. Especially, these environmental health risks will be focussed at in the next OECD Environmental outlook and its modelling approach is elaborated on.

Health modelling

30. The main purpose of the health model is to describe the burden of disease by sex and age. The methodology is a multi-state modeling approach which largely follows the approach as described in the World Health Report 2002 (WHO, 2002) and the Disease Control Priorities Project (DCPP) (Cairncross and Valdmanis, 2006). The states distinguished are exposure, disease states and death. The dynamic and integrated character of the proposed methodology is represented by the risk factor-attributable mortality and morbidity. This component is strongly connected with the socio-economic and environmental domain.

Figure 9
Overview of simple dynamics and interlinkages of the modules in GISMO

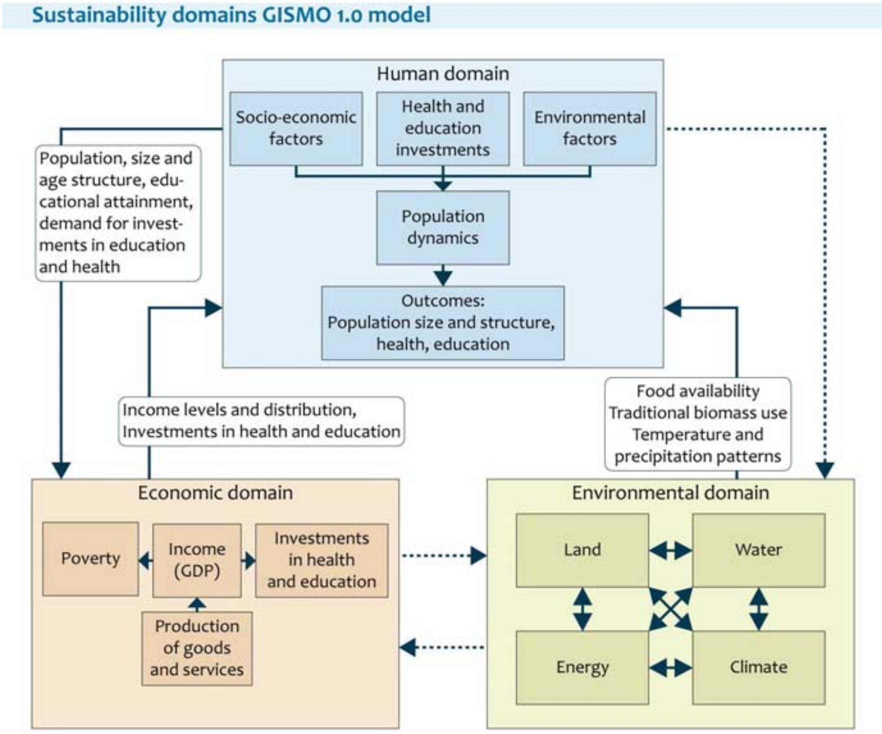

Figure 10
Multi-state modelling of cause-specific mortality

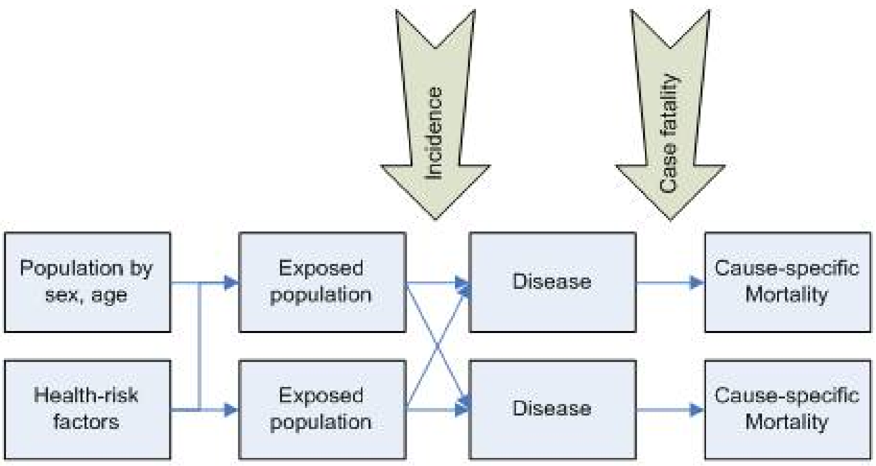

Methodology

31. For every disease included in the health module, a base incidence rate and a base case-fatality rate for all age groups and both sexes is calculated. These base levels reflect minimum levels that can only be attained by removing all exposure to risk factors and with no excess incidence or case fatality. The effect of risk factors (rf) is included by relative risk ratios (RR) on incidence rates, on case fatality rates or both. If more than one risk factor is related to a certain disease, the total effect of these risk factors is calculated in a multiplicative way. Excess incidence or case-fatality rates occur, when interregional variance still exists in risk-free rates, which are calculated by eliminating the increased risks due to risk factors. This variance can have various explanations, the most important of which is the level of health care services. For the included diseases, specific base mortality rates can be calculated by multiplying the disease-specific base incidence rates and base case-fatality rates. The individual effect of one of the relevant risk factors can be calculated as the *Population Attributable Fraction* (PAF) of that risk factor for a certain disease. Calculation and application of these fractions are described by Ezzati *et al*. (2002). Separate PAFs can be calculated for incidence (PAFI) and mortality (PAFM), showing the fraction of the incidence of mortality that can be averted, by eliminating the exposure to the risk factor in question. By summing these attributable mortality levels for all diseases related to a certain risk factor, the total attributable mortality due to that risk factor is calculated.

Included risk factors

32. Based on the described selection criteria, risk factors and their related diseases are selected to be included in the model. In Table 2, the already included risk factors and their outcomes are presented, divided in risk factor types. The outcomes relate to both disease burden and mortality due to the named diseases. Poverty is explicitly included in the model. However, most of the health loss due to impoverishment is related to other proximal and / or distal determinants. For instance, having access to improved sanitation or being educated is related to socio-economic status.

33. In the remainder of this chapter, the implemented risk factors and diseases selected for the next Environmental Outlook are described.

Table 2
Overview of the included distal, proximal and patho-physical determinants and diseases

Distal / socio-economic causes	Proximal causes	Patho-physiological causes	Outcomes
Income Education Available food per capita Temperature Precipitation Emissions	Improved water Supply Improved sanitation Malnourishment Traditional biomass use Poverty PM concentrations	Underweight	Diarrheal diseases Malaria Pneumonia / ARI Cardio-pulmonary disease Lung Cancer

Water Supply and sanitation

34. Currently, 1.1 billion people have no safe water supply and 2.4 billion people even lack basic sanitation. The vast majority of these people live in Asia and Africa. Unsafe water supply and sanitation is responsible for 5.5 percent of worldwide DALY loss, due to diarrhoeal diseases. To describe development in water supply and in sanitation levels, a path of development of various levels of WSS is used. These levels of development are adapted from the *Disease Control Priorities Project* (DCPP) (Cairncross and Valdmanis, 2006). As can be derived from box 2, it is assumed that developments in water-supply levels will be implemented ahead of developments in sanitation levels. This view is justified by data on water supply and sanitation (WSS) levels (WHO/UNICEF, 2006), from which it appears that, for almost all countries, water-supply levels are higher than sanitation levels. Separate levels of development on this path are calculated for urban and rural populations. This makes it possible to obtain variation between urban and rural diarrhoeal burden of disease. Given the state of development in the regions, total relative risk ratios are calculated, based on the "realistic scenario" used in the DCPP (Cairncross and Valdmanis, 2006) to describe the health effects of this risk factor.

Urban Air Pollution (GUAM)

35. Based on the World Bank GMAPS model, a version, called GUAM (Global Urban Air quality Model) has been developed. As GMAPS, GUAM includes demographic, geographic and meteorological conditions but instead of drivers, emissions as modelled by IMAGE are used directly. The outcomes of GUAM are twofold. First it calculates the PM10 concentration for 3300 major cities. Secondly, it calculates health effects of exposure to these concentrations. Estimation of population exposure for health impact assessments is based on the assumption 'one population – one average exposure level'. This means that it the exposure of the urban population is estimated as the modelled average urban concentration. Concentration gradients within the city (*e.g.* hot-spots), different exposure for neither different population classes nor indoor pollution have been considered. The assessment does not incorporate the effects of ambient air pollution on the population living in with less than 100 000 inhabitants and on the rural population.

36. The GUAM model has also been used for the previous Outlook, and is discussed in more detail in chapter 7. Improvements of GUAM presently under development include: exposure to other air pollutants such as ozone, expansion of the exposed population, including smaller cities and rural populations.

Indoor air pollution (REMG)

37. Lower respiratory infections (LRI), or pneumonia, cause over 2 million child deaths, annually (Mathers and Loncar, 2006). The main risk factor for these infections is indoor air pollution, caused by cooking and / or heating with solid fuels, and the effect is increased in children who are underweight. These solid fuels can be traditional biomass (such as wood, charcoal, dung and crop residue) or coal. Indoor air pollution not only causes increased risk of pneumonia mortality, but also of Chronic Obstructive Pulmonary Disease (COPD) and lung cancer. Other diseases are suspected to be related to this risk factor, but evidence for these diseases is limited and they are not included.

38. The number of people exposed to indoor air pollution is very high. Besides most African countries, South and South-east Asia also still have very high rates of solid fuel use.

39. The exposure to indoor air pollution is based on the Residential Energy Model for India (van Ruijven, 2008) which is currently being scaled up to a global coverage. The health effects of exposure to this risk factor can, however, be lowered by proper ventilation when cooking and heating. The methodology to describe the burden of disease attributable to this risk factor, is adopted from the WHO (Desai *et al.*, 2004).

Climate change and Health

40. The health impacts from climate change (not including impacts as they relate to local air pollution which is described above) are modelled through malaria (with exposures in malaria risk areas determined by temperature and precipitation), malnutrition (from reduction in food production) and temperature-related mortality (heat/cold stress) and, where possible, morbidity (*e.g.* increase in diarrhoea related to temperature). The methodology for estimating malaria is based on the MARA/ARMA model projecting climatic suitability for malaria. MARA (Mapping Malaria Risk in Africa) is a UNDP sponsored initiative which provides an atlas of malaria in Africa. The effect of climate change on food production would be modelled through IMAGE. Temperature-related mortality (heat/cold stress, diarrhoea) are based on McMichael (2004). In this methodology, overall mortality is related to distribution of daily temperatures below and above an optimal temperature to obtain excess mortality. With climate change the distribution will change and alter mortality. It is uncertain to what extent temperature-related mortality can be projected due to lack of data and ability to model heat/cold stress.

More GISMO info on: http://www.pbl.nl/en/themasites/gismo/index.html

IX GUAM – GLOBAL URBAN AIR QUALITY MODEL

Methodology Air Quality

41. Urban air quality, in particular ozone (O_3) and particulate matter (PM_{10} that is, particulate matter with an aerodynamic diameter of < 10 µm) has been assessed in more than 3000 cities worldwide with populations greater than 100 000. Given concentration-response function from epidemiological studies, the health impacts from ambient air pollution have been estimated in terms of attributable deaths and DALYs.

Urban agglomerations

42. A database of the major world cities has been taken from a recent study of the World Bank (Pandey *et al*., 2007). Projections of the population in each of the cities the period 2000-2030 are based on the average annual rate of change of the urban population at the national level (UN, 2006). Cities currently smaller than 100 000 inhabitants and fast growing cities which cross the 100 000 inhabitant threshold during the period up to 2030 are not included in the database. This implies that when in the *OECD Environmental Outlook* quantitative results are presented, these results refer only to the total urban population in the cities included in the model calculations (see Figure 11). Depending on the regional cluster 55-100% of the urban population as given in the World Urbanisation Prospects (UN, 2006) is included in the calculation. With respect to the total (rural and urban) population the coverage is 20-70 % (in 2000) and 25-75% (in 2030).

Urban air quality

43. For estimating PM_{10} concentrations starting point was the urban GMAPS- model (Global Model of Ambient Particulates, developed by the World Bank, see Pandey *et al.*, 2006; WHO 2004). This (empirical) model incorporates information on factors such as energy mix, level of economic development, demographics and meteorology. The model has been parameterised on monitoring data, mostly for the period 1996-1999, for urban background locations in more than 300 cities in 55 countries. In preliminary calculations the model was run using IMAGE-results to define the necessary input (that is, GDP, energy use, and fuel mix, where needed the data has been downscaled at the national level). These preliminary runs resulted in an unrealistic outlook for the 2030 situation. As GMAPS relates drivers (economy, energy demand) to ambient air quality it is not able to predict a decoupling between economic growth and environmental state and impact. Moreover, the fact that it has been parameterised on a relatively short period (1996-1999), makes the model less suitable for scenario outlooks over 30 years.

44. Based on the original model, a version called GUAM (Global Urban Air quality Model) has been developed at PBL. As GMAPS, GUAM includes demographic, geographic and meteorological conditions but instead of drivers, emissions as modelled by IMAGE are used directly.

44. PM10 concentrations for each city are calculated in GUAM on the basis of

- The emission density of relevant pollutants per country, in the current application emissions of carbon monoxide and secondary-PM precursors are included.
- The effective local emission of pollutants in each city and country. In the current application this term is limited to effective secondary PM-emissions. Only emissions related to energy use and to industrial processes are considered here; land-use related emissions are assumed not to give a substantial contribution in the urban area.
- Population size of cities

- Local population density of cities, assumed to be constant in time, that is, the urban area increases linear with increasing population.
- A meteorological or geographic factor for each city describing the local dispersion condition. Additional factors include heating and cooling degrees-days and two topographical factors: distance from city centre to nearest coast line and city elevation. The meteorological factors are constant in time.
- A country specific constant term.

Figure 11
Urban agglomerations included in the simulations

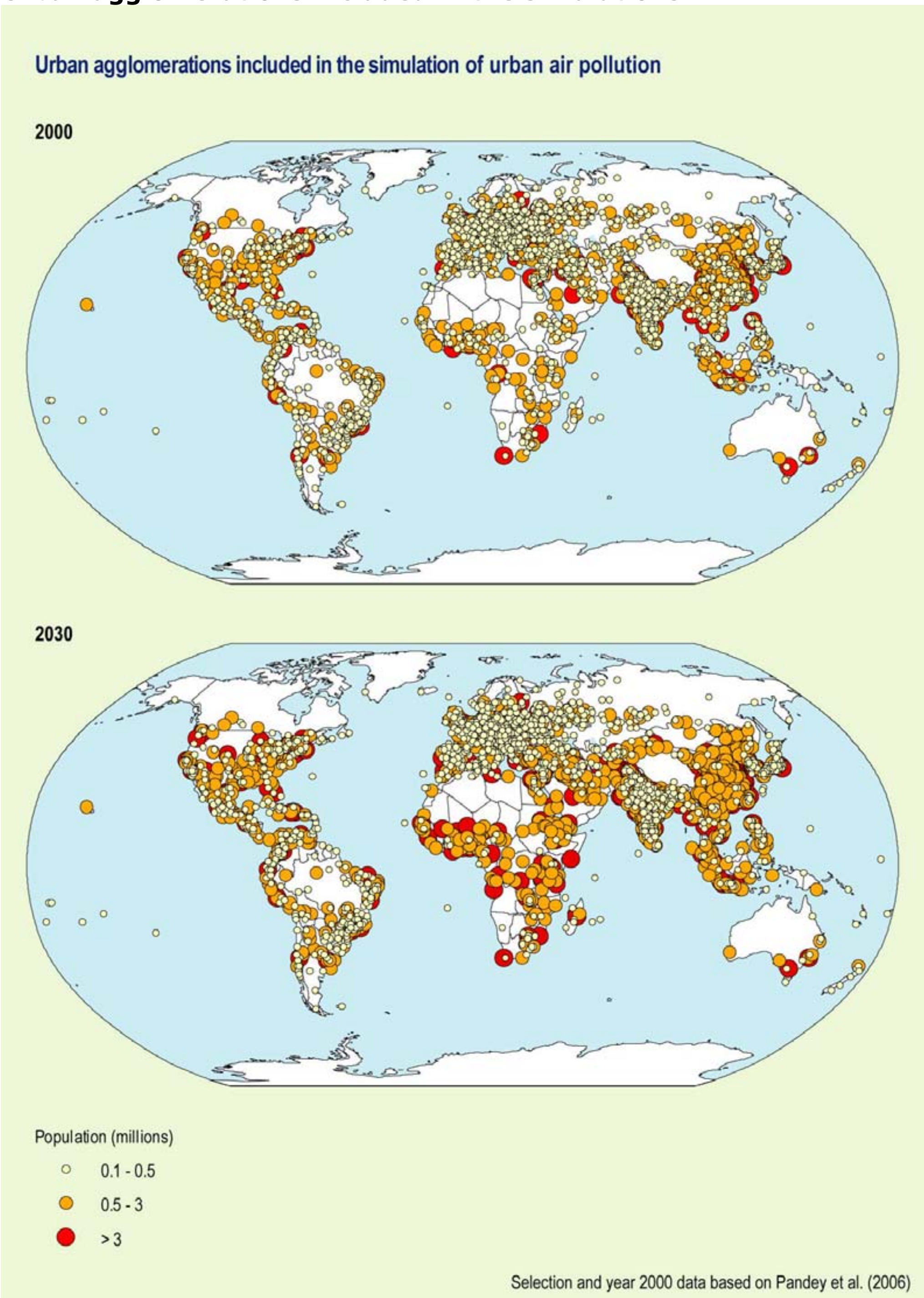

45. Background concentrations of ozone have been obtained from a global chemical tracer model (the TM3-model, Dentener *et al.*, 2005; 2006). The emissions which are used in these model calculations are based on the Current Legislation (CLE) and Maximum Feasible reduction (MFR) scenarios developed by IIASA and JRC-Ispra (Dentener *et al.*, 2005). The ozone concentration is a rather robust quantity (when the sensitivity of ozone for small changes in precursor emissions is relatively small) it is expected that the uncertainties introduced by this way are relatively small, certainly when compared to the uncertainties in the health impact assessment. The background concentrations are used as proxy for the concentration in the urban areas. This might result in a small overestimation of ozone levels as ozone concentrations tends to be lower in urbanized area due to a chemical interaction with freshly emitted nitrogen oxides.

Health Impact Assessment

46. Estimation of population exposure for health impact assessments is based on the assumption 'one population – one average exposure level'. This means that it the exposure of the urban population is estimated as the modelled average urban concentration. Concentration gradients within the city (*e.g.* hot-spots), different exposure for neither different population classes nor indoor pollution have been considered. The assessment does not incorporate the effects of ambient air pollution on the population living in cities with less than 100 000 inhabitants and on the rural population.

Table 3
Estimates of relative risk of mortality

Health outcome	**Exposure metric**	**Relative risk per 10 µg/m^3 (95% CL)**	**Reference**
Mortality from cardiopulmonary disease, adults > 30 year	PM2.5	1.059 (1.015-1.105)	Pope *et al.*, 2002
Mortality for lung cancer, adults > 30 year	PM2.5	1.082 (1.011 – 1.158)	Pope *et al.*, 2002
Mortality from acute respiratory infection, children aged 0-4 year	PM2.5	1.010 (0.991 – 1.031)	WHO, 2004
Total mortality, adults > 30 year; excluding violent death	PM10	1.043 (1.026-1.061)	Kunzli *et al.*, 2000
Total mortality, adults > 30 year, excluding violent death	ozone	1.003 (1.001 – 1.004)	WHO, 2006

47. The composition of the particulate matter will be different in the regional clusters and with changing emissions in precursors and primary PM its composition will change over time. However, we have assumed that the factors given in Table 3 have no temporal or spatial dependence.

48. Once the relative risks have been determined, the fraction of health effects from air pollution for the exposed population is calculated from the population exposure category and their relative risk.

49. In the impact assessment a constant PM2.5/PM10 ratio of 0.5 was adopted (Cohen et al. 2004). The reference concentration C_0, the theoretical minimum concentration below which there is no excess risk, is set at 15 μg/m^3 for PM10 and 7.5 μg/m3 for PM2.5. It is further assumed that for PM10 concentrations above 150 μg/m3 there is no further increase in excess risk.

50. Demographic data (total population and age distribution per country) for the period 2000-2030 has been taken from the medium fertility variant of the World Population Prospects (UN, 2005). Similar age distributions for urban and total population have been assumed. Information on baseline incidences is obtained from the WHO Burden of Disease project (Mathers and Loncar, 2006).

51. As a consequence of the uncertainties in this assessment, the quantitative results obtained cannot be confidently extrapolated to smaller geographical areas like countries or cities. Results are therefore only presented at the larger scale of regional country groupings.

X GLOBAL NUTRIENT MODEL

Point sources

52. A conceptual relationship of per capita N emission and per capita income (in Purchasing Power Parity terms) is used to calculate urban waste water N discharge, modified from (van Drecht *et al*., 2003, Bouwman *et al.* ,2005). The N-emission is calculated as annual mean per capita and country. We assume N-emission varies with GDP only. Low-income countries have per capita N emissions of about 10 g per day and industrialized countries are between 15 and 18 g per day.

53. The amount of N that is actually discharged to surface water is calculated as a function of the N emission, the rate of removal in waste water treatment plants expressed as a fraction of the N-emission in raw waste water, and the fraction of the total population connected to (public) sewerage systems.

54. In this approach we neglect waste water N emissions from rural populations. The access to improved sanitation differs between rural and urban populations. For industrialized countries the access is generally 100% for both rural and urban populations. However, in transition and developing countries the access to improved sanitation is much lower for the rural than for the urban population. Particularly in the rural areas of many developing countries, the human waste is commonly collected in latrines or septic tanks; we assume that this does not enter the surface water. However, in densely populated developing countries in the tropics with a high proportion of the population living in rural areas, the contribution of sewage Nitrogen to surface water pollution may well be significant. We do not account for coastal areas with direct discharge to the sea as far as this practice is not included in the no-treatment class.

55. For the removal of Nitrogen (R), different types of waste water treatment are distinguished (Table 4). The value for R is calculated as the weighted average of no treatment, mechanical, biological, and advanced treatment. In most developing countries the overall N removal rate is low because advanced and biological treatment are not widespread. Errors in the estimated N discharge from sewerage systems are, therefore, small. Projections for waste water treatment for 2030 are not available. We assumed that a doubling of the N-removal percentage in the period 1995-2030 must be possible. We assumed a maximum N-removal of 80%, based on current treatment technology.

Table 4
Types of sewage treatment distinguished and their nitrogen removal rates

	This study	Kristensen et al.
	%	
None	0	0
Mechanical	10	20 - 25
Biological	35	36 - 55
Advanced	80	45 - 83

OECD Environmental Outlook modelling suite, final output from IMAGE cluster, Kristensen, Fribourg-Blanc and Nixon (2004).

Table 5
Assumptions for access to improved sanitation, population with sewerage connection and nitrogen removal in sewage treatment systems

	Baseline	pp Global
S_u, access to improved sanitation (fraction of urban population)	S_u is constant, *i.e.* fraction of population with improved sanitation grows at the same rate as urbanization	50% of the gap between $S_{u,2000}$ and S_u=100% is closed in 2030
D, population connected to public sewerage (fraction of urban population)	*D* is constant, *i.e.* urban population with sewerage connection is a constant fraction of S_u	50% of the gap between D_{2000} and 100% connection in urban areas is reached in 2030
R, removal of nitrogen in sewage treatment plants (%)	50% of the gap between 2000 and the target is closed. Target is twice that in 2000 (R_{2030}=2R_{2000})[a)].	100% of the gap between 2000 and the target is closed. Target is twice that in 2000 (R_{2030}=2R_{2000})[a)].

Figure 12
Scheme of estimation of sewage nitrogen effluent to surface water

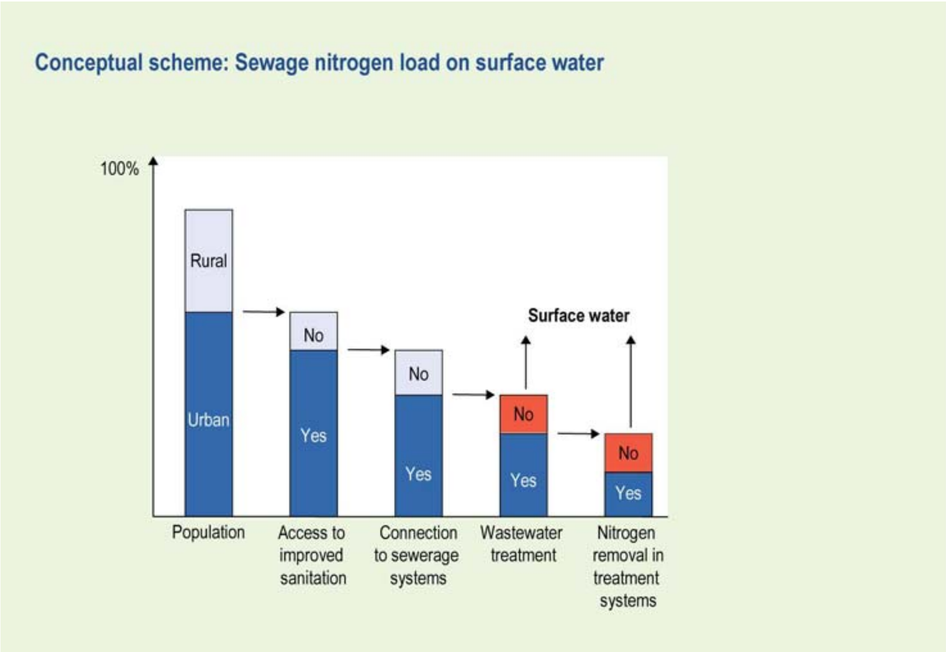

Nonpoint sources

56. Each IMAGE agricultural 0.5 by 0.5 degree gridcell consists of four aggregated agricultural land uses, including grassland, wetland rice, leguminous crops (pulses, soybeans) and other upland crops (Figure 13). The annual surface nitrogen balance includes the nitrogen inputs and outputs for each land use type. Nitrogen inputs include biological nitrogen fixation (N_{fix}), atmospheric nitrogen deposition (N_{dep}), application of synthetic nitrogen fertilizer (N_{fert}) and animal manure (N_{man}). Outputs in the surface nitrogen balance include nitrogen removal from the field by crop harvesting, hay- and grass-cutting, and grass consumption by grazing animals

(N_{exp}). The surplus of the surface nitrogen balance (N_{sur}) is calculated from these components. The different input and output terms of the surface balance are discussed in detail in various publications (Bouwman, 2005; MNP, 2006).

57. The groundwater flowing into draining surface water is a mixture of water with varying residence times in the groundwater system. The nitrate concentration in groundwater depends on the historical year of water infiltration into the saturated zone and the denitrification loss during its transport. Two groundwater subsystems are distinguished, i.e. shallow groundwater with rapid transport of nitrate in surface runoff and flow through shallow groundwater to local water courses and deep groundwater with slow transport through deep groundwater towards larger streams and rivers (Figure 14). Shallow groundwater both recharges the deep groundwater layer and discharges into local water courses.

Figure 13
Scheme of surface nitrogen balance for agricultural systems

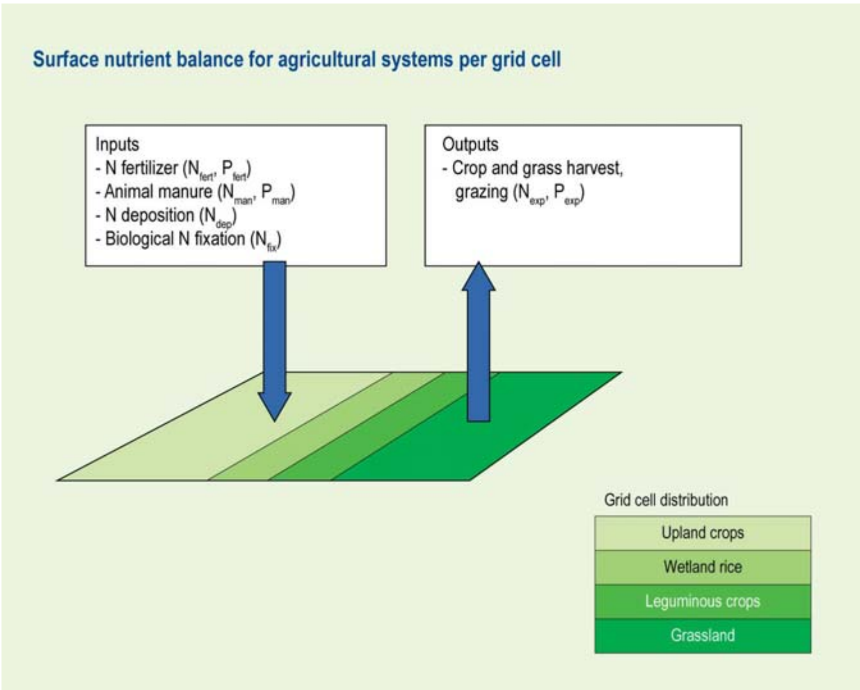

Applied within each 0.5 by 0.5 degree grid cell in IMAGE 2.4. N_{sur} is defined as the difference between nitrogen inputs and outputs according to equation (3). N_{sur} is subject to ammonia volatilization, denitrification or leaching.

River nitrogen transport

58. The total nitrogen from point sources, direct atmospheric deposition and nitrate flows from shallow and deep groundwater form input to the surface water within each grid cell. In-stream metabolic processes remove nitrogen from the stream water by transferring it to the biota, atmosphere or stream sediments. We use a global river-export coefficient of 0.7 (implying retention and loss of 30% of the nitrogen discharged to streams and rivers) which represents a mean of a wide variety of river basins in Europe and the U.S.A. used by van Drecht et al. (2003).

Figure 14
IMAGE 2.4 calculation of river nitrogen load

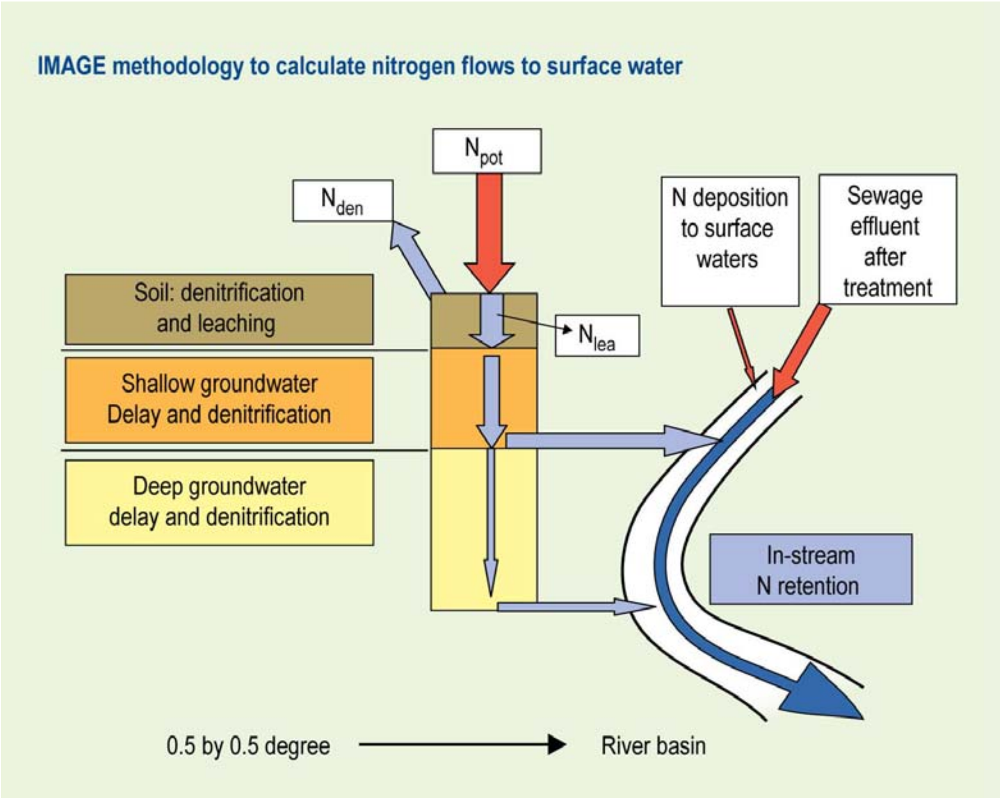

Based on van Drecht *et al.* (2003)

X GLOBIO3 – GLOBAL BIODIVERSITY MODELLING

59. According to the Convention on Biological Diversity (CBD), biodiversity encompasses the overall variety found in the living world and includes the variation in genes, populations, species and ecosystems. Several complementary indices are used within the CBD framework. In this document biodiversity loss is expressed for each biome in *the mean relative abundance of the original species* (MSA; see Box 1). In this index, the abundances of individual species are compared to their abundances in the natural or low-impacted state. Therefore, this aggregated indicator can be interpreted as a measure of 'naturalness' or 'intactness', and is similar to the Biodiversity Intactness Index BII (Scholes & Biggs, 2005).

60. The GLOBIO3 model (Alkemade *et al.*, 2009) is the successor of the Natural Capital Index module (NCI) of IMAGE (ten Brink, 2000) and the GLOBIO2 model (UNEP, 2001). The main result from the GLOBIO3 model is the relative Mean Species Abundance of originally occurring species (MSA). GLOBIO3 is built on a set of equations linking environmental drivers and biodiversity impact, so called cause–effect relationships. These relationships are derived from available literature using meta-analyses. Where possible, relationships for each driver are derived by biome – depending on the amount of available data.

61. The drivers included in the model are: *i)* land use including agriculture, forestry and built up area, and land-use intensity, *ii)* nitrogen deposition (taken from IMAGE), *iii)* infrastructure development, encroachment, *iv)* fragmentation and *v)* climate change. The relationship were constructed by firstly find relevant datasets on local species composition changes due to the specific drivers, secondly MSA values were calculated for disturbed situations by comparing the abundance or densities found in that situation with the reported undisturbed state. Finally the extracted MSA values were summarized, using a statistical model

62. For land use we found 95 datasets from many parts of the world and from different ecosystems. Land-use types were categorized into 10 classes: primary vegetation, lightly used forests, secondary forests, forest plantations, livestock grazing, man-made pastures, agro forestry, low-input agriculture, intensive agriculture, and built-up areas. The meta-analysis is now under review. For nitrogen deposition we found 22 studies on experimentally loading beyond the N critical load levels and corresponding species composition. The results are published in Bobbink *et al.*, 2010. The effect disturbance of ecosystems along roads and the effect of small scale encroachment was described using 74 datasets. A relation between MSA and the distance from roads could be estimated. The meta-analysis on the disturbance along roads is described in Benitéz-Lopéz *et al.*, 2010. For fragmentation we used 13 datasets on the minimal area requirement of animal species. The results of this analysis are shown on the above mentioned website. A meta-analysis is in preparation. For climate change we use Species Distribution Models from the EUROMOVE model (Bakkenes *et al.*, 2002) to estimate species distributions for the situation in 1995 and the forecasted situation in 2050 for three different climate scenarios. For each grid cell the proportion of remaining species were calculated by comparing the species distribution maps for 1995 and for 2050 (Bakkenes *et al.*, 2006). For each biome, a linear regression equation was estimated between the proportion of remaining species and the Global Mean Temperature Increase (GMTI), relative to pre-industrial, corresponding to the different climate scenarios. Additionally, the expected stable area for each biome calculated for different GMTIs was derived from Leemans & Eickhout (2004). They presented percentages of stable area of biomes at 1, 2, 3, and 4_Celcius GMTI. Linear regression analysis was used to relate the percentages and GMTI. Stable areas for each biome (IMAGE), or group of plant species occurring within a biome (EUROMOVE) are considered

proxies for MSA. The different relationships for biomes includes the differences in climate change projected for each biome

63. The input for the GLOBIO3 model is mainly derived from the IMAGE model, but also consist in additional data on land cover, roads and production systems. In Figure 15 the calculation scheme is given:

Figure 15
General flowchart of a GLOBIO3 analysis

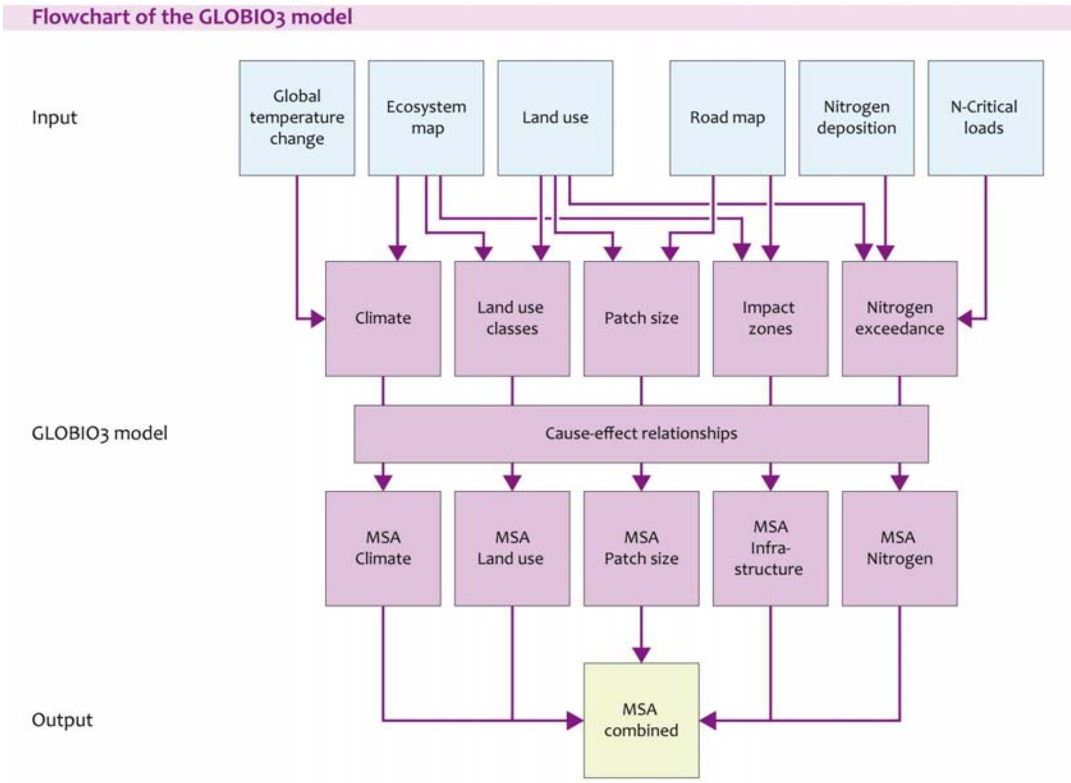

64. The input derived from IMAGE consists of the global mean temperature increase, an ecosystem or biome map, a land use map and a nitrogen deposition map. We use the Digital Chart of the world as a road map and a critical load map derived from Bouwman *et al.*, (2002). This input is used to calculate GLOBIO maps on climate, land use, patch size, infrastructure impact zones and Nitrogen exceedance. The cause-effect relationships are used to calculate the MSA for each driver and finally these MSA values are combined by so implying multiplying the separate MSA maps. Calculating MSA at regional, biome and global level is done by taking the area weighted average over all grid cells belong to a certain region. The resulting figure is an estimate for the mean abundance of the original species relative to their abundance in undisturbed ecosystems. Next to MSA the IMAGE-GLOBIO model calculates the remaining natural area of a biome ('ecosystem extent') and the remaining natural area of high quality.

GLOBIO aquatic

65. The driving forces on inland aquatic ecosystems currently included in GLOBIO are land use changes in the catchment, eutrophication by phosphorus and nitrogen, and flow changes due to water abstraction or river damming. Global warming, overfishing and possibly biological invasions will be included later. As for the terrestrial model, the 'cause-effect relationships' were

based on a meta-analyses of available literature data on species composition as a function of different degrees of the pressure (Weijters *et al.*, 2009; Alkemade *et al*., in prep.). Biodiversity was again expressed as the abundance of the original species relative to the pristine state, or a proxy for that. Separate analyses were made for shallow and deep lakes (as a function of phosphorus and nitrogen concentrations), wetlands (dependent on human land use) and rivers (dependent on both human land use and deviation from the natural flow regime). The effects of different pressures (if applicable) are assumed to be independent and hence multiplied. For lakes, also the probability of the occurrence of harmful algal blooms is calculated.

Box 1: The Biodiversity indicator MSA

Mean species abundance is not an absolute measure of biodiversity. If the indicator value is 100%, the biodiversity is similar to the natural or low-affected state. If the indicator value is 50%, the average abundance of original species is 50% of the natural or low-affected state, and so on. By definition, the abundance of exotic or invasive species is not included in the indicator, but their impact shows by the decrease in the abundance of the original species they replace.

As a result of human activities, different ecosystem types are often becoming more and more alike. This is sometimes referred to as 'levelling out' or 'homogenization' of biodiversity (ten Brink, 2000; Pauly, 1998; Scholes and Biggs, 2005; MEA, 2005). Strongly expanding species, which may sometimes even become plagues in terms of invasions and infestations, are a signal of both biodiversity loss and decreasing populations. The graphs below illustrate the difference between an intact, rich ecosystem (left) and a degraded ecosystem (right). The individual species abundances in the left hand graph reflect the (indexed) natural population sizes for a variety of species that span the range for an intact system (shaded area). In contrast, the abundance of most species in the middle and right hand graphs have dropped below this range, reflecting a loss of species and a skewed distribution of population sizes. The calculated MSA indicator values (black horizontal lines) drop from left to right, reflecting the homogenization process.

MSA can be specified for geographical regions and different nature types (or biomes). The MSA values at the global and regional levels are the sum of the underlying biome values (in km^2) in which the abundances for each biome are equally weighted (ten Brink, 2000; UNEP, 2003).The contribution of different causes of loss can be distinguished, which offers the opportunity to assess the effects of policy options targeted at pressures. The indicator is very suitable for use in comparing different future projections that give developments in direct and indirect drivers related to the distinguished pressures (PBL, 2010).

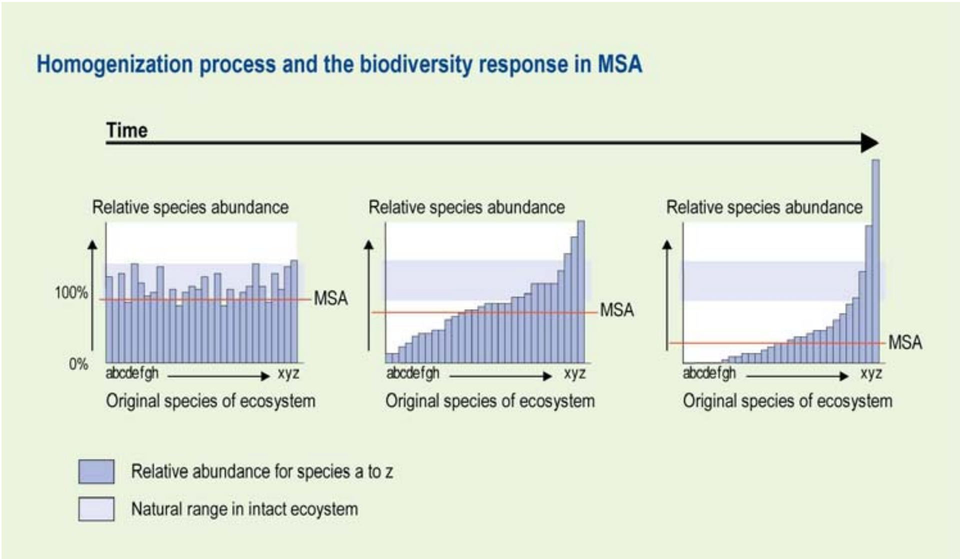

The various nature types in the world, also called 'biomes' vary greatly in the number of species, their species composition and their species abundance. Obviously a tropical rainforest is entirely different from tundra or polar systems. A key feature is that the indicator treats the biodiversity value of all ecosystems alike, whether tundra or tropical rainforest. Thus, the indicator allows aggregation and projection into the future only because it is a crude measure.

By equally weighing, no additional value is assigned to endangered ecosystems. The MSA indicator is not intended to highlight individual species under threat. Lastly, aggregation across regions may also mask differences between regions or biomes by averaging.

It should be emphasized that the presented results are rough estimates only and based on pressures that are model outcomes in themselves, instead of monitored pressures. In reality, impacts of the various pressures are probably not independent but are interacting. Furthermore, effects related to climate change are long-term, *i.e.* the consequence of slowly changing species composition. In fact, in ecosystems in the northern regions, which are at present already under significantly large pressure from the current rate of climate change, the modeled climate change effects have not yet materialized (ten Brink, 2000).

Vice versa, when pressures decrease, the model will show a fast recovery in biodiversity. In reality, restoration will take a considerable amount of time. Analysis of the GLOBIO literature database on secondary forest growth showed that a full recovery of biodiversity (in MSA) is not likely within 50 years, with distinct differences in species groups (birds, plants, insects). In 50 years, biodiversity converges to an MSA value around 0.5. The recovery of specific canopy species will take more than 100 years. This long period for full recovery is the consequence of the complex vertical layered structure of especially tropical forests, and the slow growth rates of trees that dominate the climax situation (Peña-Claros, 2003).

Complete recovery in abandoned agricultural areas to natural grassland ecosystems may be faster than for forests, as their vertical structure is less complex. Restoration of low productive heathlands on former agricultural fields was especially difficult for rare plant species, while insects responded much more quickly (Verhagen, 2007). The recovery process could not be completely analyzed with the literature contained in the current GLOBIO database.

XII EDGAR – IMAGE EMISSIONS DATABASE

67. To provide the input data for TIMER and IMAGE on energy use and historic emissions EDGAR has been used. The EDGAR (Emission Database for Global Atmospheric Research) information system is a joint project of the European Commission - JRC Joint Research Centre and PBL Netherlands Environmental Assessment Agency as part of and in cooperation with the *Global Exchange and Interactions Activity* (GEIA) of IGBP and the *ACCENT Network of Excellence*. EDGAR stores global emission inventories of direct and indirect greenhouse gases from anthropogenic sources including halocarbons and aerosols both on a per country and region basis as well as on grid. EDGAR serves as reference database, worldwide, for policy applications as well as for scientific studies by providing gridded emissions as input for atmospheric models (Olivier and Berdowski, 2001; http://www.pbl.nl/edgar).

68. EDGAR includes the following sources: *(a)* fossil-fuel related sources and *(b)* biofuel combustion, both on a per country basis; *(c)* industrial production and consumption processes (including solvent use) also on a per country basis; *(d)* landuse-related sources, including waste treatment, partially on a grid basis and partially on a per country basis; and *(e)* selected natural sources on a grid basis. The level of detail per source is generally defined by the available international statistics (*e.g.* for fuel combustion the many fuel types and economic subsectors distinguished by the IEA statistics).

69. The inventories are not stored as emissions but are calculated per source category, firstly at country level by multiplication of *(a)* activity data (in general international statistics) and *(b)* emission factors (for greenhouse gases in general IPCC default values). Subsequently, emissions at a 1x1 and 0.1 x 0.1 degree grid may be generated from the emissions at country level using source-specific global grid maps as proxy for the spatial distribution of emissions within countries. Aircraft emissions are also calculated at 1 km altitude bands. The EDGAR system can generate global, regional and national emissions data in various formats for any definition of source categories.

70. Activity data were mostly taken from international statistical data sources and emission factors were selected mostly from international publications to ensure a consistent approach across countries (Olivier *et al*., 2006; Olivier *et al*., 2005, Van Aardenne *et al.*, 2001).

71. All activity data are available in detail for 1970-2008 (annually) and at more aggregate level for 1880-1990 (per 10 year). Emission factors also cover these periods, except for air pollutants (NOx, CO,NMVOC, SO_2) for which no detailed factors are available for 1970-1985. For all compounds and standard source categories emissions were calculated for 1970 - 2008.

72. The uncertainty in the resulting dataset at national level may be substantial, especially for methane and nitrous oxide, and even more so for the F-gases. The uncertainty is caused by the limited accuracy of international activity data used and in particular of emission factors selected for calculating emissions on a country level. However, since methods used are comparable with IPCC methodologies and global totals comply with budgets used in atmospheric studies and the data were based on international information sources, this dataset provides a sound basis for comparability. Details on uncertainty and caveats identified in the dataset, as well as more detailed source category estimates are available at the website (see also: Olivier *et al*., 2001, and Olivier and Peters, 2002).

73. The *OECD Environmental Outlook* addresses several aspects of conventional air pollution including emissions of sulphur dioxide, nitrogen oxides, airborne particulate matter and ground

level ozone. The focus is on what the Baseline and policy measures mean for urban air quality worldwide, and the associated health and human development impacts.

74. Ambient particulate matter is partly directly emitted into the atmosphere (dominant sources are fossil fuel use, wood burning and road transport); partly it is formed in the atmosphere from precursor gases (sulphur dioxide, nitrogen oxides, ammonia and, to a lesser extent, volatile organic compounds). Ground-level ozone is a secondary pollutant: it is not directly emitted but formed in the atmosphere. Important precursors of ozone are nitrogen oxides, volatile organic compounds, methane and carbon monoxide.

75. Future emissions of sulphur dioxide, nitrogen oxides, methane and carbon monoxide from the energy system are calculated by IMAGE/TIMER using a system of sector/region/substance specific emission coefficients (based on the EDGAR database), calibrated to historic trends. Land use related emissions are calculated in a similar manner based on the land use and agricultural parameters like intensity, fertilizer and manure application, animal diets and feed efficiency, etc.

More EDGAR information on: http://edgar.jrc.ec.europa.eu

References

Alcamo, J., Kreileman, G. J. J., Krol, M. S. & Zuidema, G. (1994) Modeling the global society-biosphere-climate system: Part 1: Model description and testing. *Water, Air, and Soil Pollution*, 76, 1-37.

Alcamo, J., Leemans, R. & Kreileman, G. J. J. (1998) *Global change scenarios of the 21th century; results from the IMAGE 2.1 model*. Pergamon, Elsevier Science Ltd., Oxford, UK.

Alkemade, R., Van Oorschot, M., Miles, L., Nellemann, C., Bakkenes, M. & Ten Brink, B. (2009) GLOBIO3: A framework to investigate options for reducing global terrestrial biodiversity loss. *Ecosystems*, 12: 374-390. doi: http://dx.doi.org/10.1007/s10021-009-9229-5

Alkemade R. Janse J. Van Rooij W. Trisurat Y. (2011) *Applying GLOBIO at different geographical levels*. in: Trisurat Y., Shrestha R., Alkemade R. (eds.) Land use, climate change and biodiversity modelling. IGI Global, Hershey PA, USA.

Bakkenes, M., Alkemade, J.R.M., Ihle, F., Leemans, R., Latour, J.B. (2002), Assessing effects of forecasted climate change on the diversity and distribution of European higher plants for 2050, *Global Change Biology* 8(4): 390-407.

Bakkenes, M. , Eickhout, B. , Alkemade, R. (2006), Impacts of different climate stabilisation scenarios on plant species in Europe, *Global Environmental Change* 16(1) 19-28.

Banse M., van Meijl H., Tabeau A. and Woltjer G. (2008). Will EU Biofuel Policies Affect Global Agricultural Markets? *European Review of Agricultural Economics*, 35(2):117–141.

Benítez-Lópeza, A., R. Alkemadea, P.A. Verweij (2010) The impacts of roads and other infrastructure on mammal and bird populations: A meta-analysis, *Biological Conservation*, 143 (6): 1307–1316.

Biemans, H., R. W. A. Hutjes, P. Kabat, B. J. Strengers, D. Gerten, S. Rost (2009). Effects of Precipitation Uncertainty on Discharge Calculations for Main River Basins. *J. Hydrometeor*, 10: 1011–1025. doi: http://dx.doi.org/10.1175/2008JHM1067.1

Bobbink, R., K. Hicks, J. Galloway, T. Spranger, R. Alkemade, M. Ashmore, M. Bustamante, S. Cinderby, E. Davidson, F. Dentener, B. Emmett, J-W. Erisman, M. Fenn, F. Gilliam, A. Nordin, L. Pardo, and W. De Vries (2010). Global assessment of nitrogen deposition effects on terrestrial plant diversity: a synthesis. *Ecological Applications* 20:30–59. http://dx.doi.org/10.1890/08-1140.1 .

Bondeau, A., Smith, P. C., Zaehle, S., Schaphoff, S., Lucht, W., Cramer, W., Gerten, D., Lotze-Campen, H., Müler, C., Reichstein, M. and Smith, B. (2007), Modelling the role of agriculture for the 20th century global terrestrial carbon balance. *Global Change Biology*, 13: 679–706. doi: http://dx.doi.org/10.1111/j.1365-2486.2006.01305.x

Bouwman, A.F., Van Vuuren, D.P., Derwent, R.G., Posch, M. (2002), A global analysis of acidification and eutrophication of terrestrial ecosystems. *Water, Air, and Soil Pollution* 141(1-4): 349-382.

Bouwman, A.F., Van Drecht, G., Van der Hoek, K.W., (2005). Surface N balances and reactive N loss to the environment from intensive agricultural production systems for the period 1970-2030, *Science in China Ser. C. Life Sciences*, pp. 1-13.

Bouwman, A.F., Klein Goldewijk, K., Van der Hoek, K.W., Beusen, A.H.W., Van Vuuren, D.P., Willems, W.J., Rufino, M.C., Stehfest, E. (2011). Exploring global changes in nitrogen and phosphorus cycles in agriculture induced by livestock production over the 1900-2050 period.

Proceedings of the National Academy of Sciences of the United States of America, http://dx.doi.org/10.1073/pnas.1012878108.

Brink, B.J.E. ten (2000), *Biodiversity Indicators for the OECD Environmental Outlook and Strategy, a Feasibility Study*, RIVM National Institute for Public Health and the Environment, in co-operation with WCMC, Cambridge/Bilthoven.

Bruinsma, J.E. (2003), *World agriculture: towards* 2015/2030. An FAO perspective, Earthscan, London.

Burniaux, J. M. and T.P. Truong (2002) GTAP-E: an Energy–Environmental Version of the GTAP model, *GTAP Technical Paper*, No. 16. Revised Version. Center for Global Trade Analysis, Purdue University.

Burniaux, J-M., G. Nicoletti and J. Oliveira Martins (1992), GREEN: A Global Model for Quantifying the Costs of Policies to Curb CO2 Emissions, OECD Economic Studies, 19 (Winter).

Burniaux, J. and J. Chateau (2011), Mitigation Potential of Removing Fossil Fuel Subsidies: A General Equilibrium Assessment, OECD Economics Department Working Papers, No. 853, OECD Publishing. doi: 10.1787/5kgdx1jr2plp-en.

Burniaux, J., J. Chateau and R. Duval (2010), Is there a Case for Carbon-Based Border Tax Adjustment?: An Applied General Equilibrium Analysis, OECD Economics Department Working Papers, No. 794, OECD Publishing. doi: 10.1787/5kmbjhcqqk0r-en.

Cairncross, S.; Valdmanis, V. (2006), *Water supply, sanitation and hygiene promotion* (Chapter 41). in 'Disease Control Priorities in Developing Countries' Jamison, D. T.; Breman, J. G.; Measham, A. R; et al, The World Bank (Washington DC) :771-792

Chateau, J., R. Dellink, E. Lanzi and B. Magne (2012), "An overview of the ENV-Linkages model – version 3", OECD Environment Working Paper.

Cohen, D.D., Garton, D., Stelcer, E., Hawas, O., Wang, T., Poon, S., Kim, J., Choi, B.C., Oh, S.N, Shin, H.-J, Ko, M.Y, Uematsu, M. (2004), Multielemental analysis and characterization of fine aerosols at several key ACE-Asia sites, *Journal of Geophysical Research D*: *Atmospheres*, 109(19): D19S12 1-18.

CPB (1999), Worldscan: the Core Version, CPB Netherlands Bureau for Economic Policy Analysis, The Hague, the Netherlands.

Dellink, R.B., S. Jamet, C. Chateau and R. Duval (2010), Towards global carbon pricing: direct and indirect linking of carbon markets, OECD Environment Working Paper 20, Paris.

Dellink, R., G. Briner and C. Clapp (2010b), Costs, Revenues, and Effectiveness of the Copenhagen Accord Emission Pledges for 2020, OECD Environment Working Papers, No. 22, OECD Publishing.
doi: 10.1787/5km975plmzg6-en

den Elzen MGJ and Lucas P (2003), FAIR 2.0 - A decision-support tool to assess the environmental and economic consequences of future climate regimes, RIVM report 550015001/2003, National Insitute for public Health and the Environment (RIVM), Bilthoven, The Netherlands.

den Elzen and Paul L. Lucas (2005), The FAIR model: A tool to analyse environmental and costs implications of regimes of future commitments. *Environmental Modeling and Assessment*, 10 (2): 115-134,
doi: http://dx.doi.org/10.1007/s10666-005-4647-z .

den Elzen, M.G.J. and, Van Vuuren, D.P. (2007), peaking profiles for achieving long-term temperature targets with more likelihood at lower costs, *Proceedings of the National Academy of Sciences of the United States of America*, 14(46) :17931-17936

den Elzen, MGJ, Lucas, P and van Vuuren, DP. (2008), 'Regional abatement action and costs under allocation schemes for emission allowances for achieving low CO2-equivalent concentrations', *Climatic Change* 90 (3): 243–268.

den Elzen, Michel and Höhne, Niklas (2010), Sharing the reduction effort to limit global warming to 2°C, *Climate Policy*, Volume 10, Number 3, 2010 , pp. 247-260(14)

den Elzen, MGJ, Hof, AF, Mendoza Beltran, A, Grassi, G, Roelfsema, M, van Ruijven, BJ, van Vliet, J and Van Vuuren, DP. (2011), 'The Copenhagen Accord: Abatement costs and carbon prices resulting from the submissions', *Environmental Science & Policy* 14 28-39.

Dentener, F., Stevenson, D., Cofala, J., Mechler, R., Amann, M., Bergamaschi, P., Raes, F., Derwent, R. (2005), The impact of air pollutant and methane emission controls on tropospheric ozone and radiative forcing: CTM calculations for the period 1990-2030, *Atmospheric Chemistry and Physics* 5(7):1731-1755

Dentener, F., Kinne, S., Bond, T., Boucher, O., Cofala, J., Generoso, S., Ginoux, P., Gong, S., Hoelzemann, J.J., Ito, A., Marelli, L., Penner, J.E., Putaud, J.-P., Textor, C., Schulz, M., Van Der Werf, G.R., Wilson, J. (2006), Emissions of primary aerosol and precursor gases in the years 2000 and 1750 prescribed data-sets for AeroCom, *Atmospheric Chemistry and Physics* 6(12): 4321-4344.

Desai, M. A., S. Mehta and K. R. Smith (2004). *Indoor smoke from solid fuels: Assessing the environmental burden of disease at national and local levels*. Environmental burden of disease series No. 4. D. C.-L. Annette Prüss-Üstün, Carlos Corvalán, Alistair Woodward. Geneva, Switzerland, WHO.

de Vries B; Vuuren D van ; Elzen M den ; Janssen M (2001), The Timer IMage Energy Regional (TIMER) Model, Report no. 461502024, National Institute for Public Health and the Environment (RIVM), Bilthoven.

Duval, R. and C. de la Maisonneuve (2009), Long-Run GDP Growth Scenarios for the World Economy, OECD Economics Department Working Paper 663, February 2009.

Eickhout B., van den Born G.J., Notenboom J., van Oorschot M., Ros J.P.M., van Vuuren D.P. and Westhoek H.J. (2008) Local and Global Consequences of the EU Renewable Directive for Biofuels: Testing the Sustainability Criteria. MNP Report 500143001/2008. Bilthoven, The Netherlands.

Ezzati, M., S. Vander Hoorn, A. D. Lopez, G. Danaei, A. Rodgers, C. D. Mathers and C. J. L. Murray (2002). Chapter 4: Comparative Quantification of Mortality and Burden of Disease Attributable to Selected Risk Factors. In: Global Burden of Disease and Risk Factors. A. D. Lopez, C. D. Mathers, M. Ezzati, D. T. Jamison and C. J. L. Murray (eds), A co-publication of Oxford University Press and The World Bank.

FAO (1978-81). Report on the agro-ecological zones project. World Soil Resources Report 48, FAO, Rome.

FAO-Aquastat: http://www.fao.org/nr/water/aquastat/main/index.stm

Freydank, K. and S. Siebert (2008), Towards mapping the extent of irrigation in the last century: a time series of irrigated area per country. Frankfurt Hydrology Paper 08, Institute of Physical Geography, University of Frankfurt, Frankfurt am Main, Germany.

GTAP (2008), Global Trade, Assistance, and Production : The GTAP 7 Data Base, Narayanan, B. and Walmsey, T. Editors, Center for Gloabal Trade Analysis, Dpt of Agriculutural Economics, Purdue University.

Gerten, D., S. Schaphoff, U. Haberlandt,W. Lucht, S. Sitch (2004), Terrestrial vegetation and water balance: hydrological evaluation of a dynamic global vegetation model. *Journal of Hydrology* 286: 249–270.

Hendriks C., Graus W. and F. Van Bergen (2002), Global carbon dioxide storage potential and costs. Report EEP-02001, Ecofys, Utrecht.

Hendriks C., Harmelink M., Burges K. and Ransel K. (2004), Power and heat productions: plant developments and grid losses. Report EEP-03038, Ecofys, Utrecht.

Hilderink H. and P. Lucas (eds)(2008), Towards a global Integrated sustainability model: GISMO 1.0 status report. Netherlands Environmental Assessment Agency, Bilthoven, The Netherlands.

Hermosilla, S.G.; Silvis, H.J.; Woltjer, G.B. (2010) Links between energy and food markets: a preliminary assessment, Den Haag : LEI Wageningen UR, (LEI Rapport / Research Area Natural Resources 2010-032).

Hertel, T.W. (Ed.) (1997) *Global Trade Analysis: Modeling and Applications*, Cambridge University Press.

Hilderink, H. (2000), *World population in transition: An integrated regional modeling framework*. Phd-thesis, Thela thesis, Amsterdam. pp. 256.

Hoogwijk M. (2004a), On the global and regional potential of renewable energy sources. PhD thesis, Utrecht University, Utrecht, 256 pp.

Hoogwijk, M., B. de Vries, W. Turkenburg (2004b), Assessment of the global and regional geographical, technical and economic potential of onshore wind energy. *Energy Economics* 26(5): 889-919.

Höhne, N. , den Elzen, M Weiss (2006), Common but differentiated convergence (CDC): A new conceptual approach to long-term climate policy, *Climate Policy* 6(2): 181-199.

International Energy Agency (2009a), *World Energy Outlook 2009*, OECD Publishing. doi: 10.1787/weo-2009-en.

International Energy Agency (2010a), *CO2 Emissions from Fuel Combustion 2010*, OECD Publishing. doi: 10.1787/9789264096134-en.

International Energy Agency (2010), *World Energy Outlook 2010, OECD Publishing*. doi: 10.1787/weo-2010-en.

International Energy Agency (2009b), *Energy Technology Perspectives 2010: Scenarios and Strategies to 2050*, OECD Publishing.
doi: 10.1787/energy_tech-2010-en.

IEA, OPEC, OECD, World Bank (2010), Analysis of the Scope of Energy Subsidies and Suggestions for the G-2) initiative, Joint Report prepared for submission to the G-20 Meeting of the Finance Ministers and Central Bank Governors, Busan (Korea), 5 June 2010, 26 May 2010.

IMAGE Team (2001), The IMAGE 2.2 Implementation of the SRES Scenarios. A Comprehensive Analysis of Emissions, Climate Change and Impacts in the 21st Century (RIVM CD-ROM publication 481508018), National Institute for Public Health and the Environment, Bilthoven.

IMF(2010), ‘World Econonomic Outlook Database’, http://www.imf.org/external/pubs/ft/weo/2010/02/weodata/index.aspx

Kristensen, Fribourg-Blanc and Nixon (2004), Outlooks on nutrient discharges in Europe from urban waste water treatment plants, European Environment Agency, Eur. Topic Cent. on Water, Copenhagen.

Künzli, N., Kaiser, R., Medina, S., Studnicka, M., Chanel, O., Filliger, P., Herry, M., Horak Jr., F., Puybonnieux-Texier, V., Quénel, P., Schneider, J., Seethaler, R., Vergnaud, J.-C., Sommer, H. (2000), Public-health impact of outdoor and traffic-related air pollution: A European assessment, *Lancet* 356(9232): 795-801.

Leemans, R., Eickhout, B., Strengers, B., Bouwman, L. & Schaeffer, M. (2002), The consequences for the terrestrial carbon cycle of uncertainties in land use, climate and vegetation response in the IPCC SRES scenarios. *Sci. China*, 45, 126-141.

Leemans, R., Eickhout, B. (2004), Another reason for concern: Regional and global impacts on ecosystems for different levels of climate change, *Global Environmental Change* 14(3):219-228.

Mathers, CD and D Loncar (2006), Projections of global mortality and burden of disease from 2002 to 2030, *PLoS Med* 3(11): e442. doi:10.1371/journal.pmed.0030442.

McMichael, P. 2004. Third Worldism and lineages of global fascism: neo-liberalism and the regrouping of the global South. Third World Quarterly ,25(1): 231–254.

MEA (2005), Millennium Ecosystem Assessment, 2005. *Ecosystems and Human Well-being: Synthesis*. Island Press, Washington, DC.

Minnen, J. van, R. Leemans and F. Ihle (2000), Defining the Importance of Including Transient Ecosystem Responses to Simulate C-cycle Dynamics in a Global Change Model, *Global Change Biology*, 6:595-612.

MIT (2003) The future of nuclear power - an interdisciplinary MIT study. Massachusetts Institute of Technology, Cambridge MA, 180 pp.

MNP (2006), Integrated modelling of global environmental change. An overview of IMAGE 2.4. Bouwman, A. F., Kram, T. & Klein Goldewijk, K. (eds.), pp 228. Netherlands Environmental Assessment Agency, Bilthoven, The Netherlands.

Mulders, F., Hettelar, J. F. van Bergen (2006), Assessment of the global fossil fuel reserves and resources for TIMER. TNO report, TNO Built Environment and Geosciences, Utrecht, The Netherlands.

Nowicki, P., van Meijl H., Knierim A., Banse M., Helming J., Margraf O., Matzdorf B., Mnatsakanian R., Reutter M., Terluin I., Overmars K., Verhoog C., Weeger C., Westhoek H. (2007) Scenar 2020 - Scenario study on agriculture and the rural world. European Commission, Directorate-General Agriculture and Rural Development, Brussels.

OECD (2008), OECD Environmental Outlook to 2030, OECD Publishing.
doi: 10.1787/9789264040519-en.

OECD (2009), The Economics of Climate Change Mitigation: Policies and Options for Global Action beyond 2012, OECD Publishing.
doi: 10.1787/9789264073616-en.

OECD (2010), "OECD Economic Outlook No. 88", OECD Economic Outlook: Statistics and Projections (database). doi: 10.1787/data-00533-en.

Olivier, J.G.J., J.J.M. Berdowski, J.A.H.W. Peters, J. Bakker, A.J.H. Visschedijk en J.-P.J. Bloos (2001b) Applications of EDGAR. Including a description of EDGAR 3.0: reference database with trend data for 1970-1995. RIVM, Bilthoven. RIVM report no. 773301 001/ NOP report no. 410200 051.

Olivier, J.G.J. and J.J.M. Berdowski (2001) *Global emissions sources and sinks*. In: Berdowski, J., Guicherit, R. and B.J. Heij (eds.), The Climate System, pp. 33-78. A.A. Balkema Publishers/Swets & Zeitlinger Publishers, Lisse, The Netherlands. ISBN 90 5809 255 0.

Olivier, J.G.J., J.J.M. Berdowski, J.A.H.W. Peters, J. Bakker, A.J.H. Visschedijk and J.P.J. Bloos (2001) *Applications of EDGAR. Including a description of EDGAR V3.0: reference database with trend data for 1970-1995*. RIVM report 773301 001 / NRP report 410200 051. ISBN 90-5851-077-8.

Olivier, J.G.J. and J.A.H.W. Peters (2002) *Uncertainties in global, regional and national emission inventories***.** In: Van Ham, J., A.P.M. Baede, R. Guicherit and J.F.G.M. Williams-Jacobse (eds.):'Non-CO_2 greenhouse gases: scientific understanding, control options and policy aspects. Proceedings of the Third International Symposium, Maastricht, Netherlands, 21-23 January 2002', pp. 525-540. Millpress Science Publishers, Rotterdam. ISBN 90-77017-70-4.

Olivier, J.G.J., Van Aardenne, J.A., Dentener, F., Pagliari, V., Ganzeveld, L.N. and J.A.H.W. Peters (2005) Recent trends in global greenhouse gas emissions: regional trends 1970-2000 and spatial distribution of key sources in 2000**.** *Env. Sc.*, **2** (2-3), 81-99. DOI: 10.1080/15693430500400345.

Olivier, J.G.J., T. Pulles and J.A. van Aardenne (2006) Part III: Greenhouse gas emissions: 1. Shares and trends in greenhouse gas emissions; 2. Sources and Methods; Greenhouse gas emissions for 1990, 1995 and 2000. In: "*CO_2 emissions from fuel combustion 1971-2004*", 2006 Edition, pp. III.1-III.41. International Energy Agency (IEA), Paris. ISBN 92-64-10891-2 (paper) 92-64-02766-1 (CD ROM) (2006).

Pandey, K.D. D. Wheeler, B. Ostro, U. Deichmann, K. Hamilton, K. Bolt, (2006) *Ambient Particulate Matter Concentrations in Residential and Pollution Hotspot areas of World Cities: New Estimates based on the Global Model of Ambient Particulates (GMAPS)*, The World Bank Development Economics Research Group and the Environment Department Working Paper, The World Bank, Washington DC.

PBL (2010). Rethinking Global Biodiversity Strategies. PBL Netherlands Environmental Assessment Agency, The Hague/Bitlhoven, 2010.

Peña-Claros, M. (2003), Changes in Forest Structure and Species Composition during Secondary Forest Succession in the Bolivian Amazon. *Biotropica*, 35: 450–461. doi: 10.1111/j.1744-7429.2003.tb00602.x

Prentice, I.C., et al. (1992), A global biome model based on plant physiology and dominance, soil properties and climate, *Journal of Biogeography*, 19:117-134.

Pope III, C.A., Burnett, R.T, Thun, M.J., Calle, E.E., Krewski, D., Ito, K., Thurston, G.D. (2002), Lung cancer, cardiopulmonary mortality, and long-term exposure to fine particulate air pollution, *Journal of the American Medical Association* 287(9): 1132-1141.

Rogner, H.-H. (1997) An Assessment of World Hydrocarbon Resources, *Annual Review of Energy and the Environment*, 22: 217-262.

Rost, S., Gerten, D., Heyder, U. (2008), Human alterations of the terrestrial water cycle through land management. *Advances in Geosciences*, 18, 43-50.

Rotmans, J. (1990), *IMAGE. An Integrated Model to Assess the Greenhouse Effect*, Kluwer Academic Publishers, Dordrecht.

Shiklomanov, I. (2000), Appraisal and Assessment of World Water Resources, *Water International*, 25(1), pp 11-32.

Schaeffer, M. and E. Stehfest (2010). *The climate subsystem in IMAGE updated to MAGICC 6.0*, PBL report 500110005, PBL Netherlands Environmental Assessment Agency, Bilthoven, The Netherlands.

Schlesinger, M.E. et al. (2000), Geographical Distributions of Temperature Change for Scenarios of Greenhouse Gas and Sulphur Dioxide Emissions, *Technological Forecasting and Social Change* 65, 167-193.

Scholes, R.J. and R. Biggs (2005), A biodiversity intactness index, *Nature* 434: 45-49.

Sims, R.E.H., Rogner, H.-H., Gregory, K. (2003), Carbon emission and mitigation cost comparisons between fossil fuel, nuclear and renewable energy resources for electricity generation, *Energy Policy* 31(13): 1315-1326.

Sitch, S., Smith, B., Prentice, I. C., Arneth, A., Bondeau, A., Cramer, W., Kaplan, J. O., Levis, S., Lucht, W., Sykes, M. T., Thonicke, K. & Venevsky, S. (2003) Evaluation of ecosystem dynamics, plant geography and terrestrial carbon cycling in the LPJ dynamic global vegetation model. Global *Change Biology*, 9, 161-185.
doi: http://dx.doi.org/10.1046/j.1365-2486.2003.00569.x

UN (2006a), *World Population Prospects: The 2006 Revision*. United Nations, New York.

UN (2006b), *World Urbanization Prospects: The 2006 Revision*. United Nations, New York.

UNEP (2001) GLOBIO. *Global methodology for mapping human impacts on the biosphere*. Report

UNEP/DEWA/TR 25. Nairobi: United Nations Environmental Programme

UNEP (2002) Global Environment Outlook 3. United Nations Environment Programme, EarthScan, London, 446 pp.

van Aardenne, J.A., Dentener, F.J., Olivier, J.G.J., Klein Goldewijk, C.G.M. and J. Lelieveld (2001) A High Resolution Dataset of Historical Anthropogenic Trace Gas Emissions for the Period 1890-1990. *Global Biogeochemical Cycles*, 15(4), 909-928.

van Drecht, G., Bouwman, A.F., Knoop, J.M., Beusen, A.H.W., Meinardi, C.R. (2003), Global modeling of the fate of nitrogen from point and nonpoint sources in soils, groundwater, and surface water, *Global Biogeochemical Cycles* 17(4): 1-26.

van Meijl H., van Rheenen T, Tabeau A, Eickhout B. (2006), The Impact of Different Policy Environments on Agricultural Land Use in Europe. *Agriculture*, *Ecosystems and Environment* 114:21-38

van Ruijven, B. J. (2008). Energy and Development - A Modelling Approach. Dept. of Science, Technology and Society, Faculty of Science. Utrecht, Utrecht University. PhD Thesis: 271.

van Ruijven, B.J., Hari, L.,van Vuuren, D.P., de Vries, B (2008), The potential role of hydrogen energy in India and Western Europe, *Energy Policy* 36(5): 1649-1665.

van Ruijven, B., J-F. Lamarque, D.O. van Vuuren, T.,Kram, H. Eerens, H. (2011) Emission scenarios for a global hydrogen economy and the consequences for global air pollution, *Global Environmental Change* 21(3): 983-994.

van Vliet, J, den Elzen, MGJ and D.P. van Vuuren (2009), 'Meeting radiative forcing targets under delayed participation', *Energy Economics* 31 (SUPPL. 2): S152-S162.

Verhagen (2007), Changing land use: restoration perspectives of low production communities on agricultural fields after top soil removal. Dissertation, University of Groningen.

von Bloh, W., S. Rost, D. Gerten, and W. Lucht, 2010. Efficient parallelization of a dynamic global vegetation model with river routing. *Environmental Modelling & Software* 25, 685-690.

van Vuuren, D.P. (2007), Energy Systems and Climate Policy, PhD thesis, Utrecht University.

Weijters, M.J., Janse, J.H., Alkemade, R. & Verhoeven, J.T.A. (2009). Quantifying the effect of catchment land-use and water nutrient concentrations on freshwater river and stream biodiversity*. Aquat. Cons.: Mar. Freshw. Ecosyst*. 19: 104-112.

Wischmeier, W. H. and Smith, D. D. 1978. Predicting rainfall-erosion losses. A guide to conservation planning. Agricultural Handbook no. 537. U.S. Dep. Agric., Washington, D.C.

WHO (2002), *The World Health Report 2002 - Reducing Risks, Promoting Healthy Life*. World Health Organization, Geneva, Switzerland.

WHO (2004), *The World Health Report 2004 - Changing history*. World Health Organization, Geneva, Switzerland.

WHO (2006), *The World Health Report 2006 - Working together for health*. World Health Organization, Geneva, Switzerland.

WHO/UNICEF (2006). Meeting the MDG drinking water and sanitation target: the urban and rural challenge of the decade. Geneva, Switzerland, Joint Water Supply and Sanitation Monitoring Programme, World Health Organization, and UNICEF.

World Bank (2010), *World Development Indicators*, http://data.worldbank.org/data-catalog/world-development-indicators.

Annex A – World regions in the IMAGE model suite